

MELISSA

Memorandum of Understanding
ECT/FG/MMM/97.012
ESA/ESTEC Contract 12924/98/NL/MV

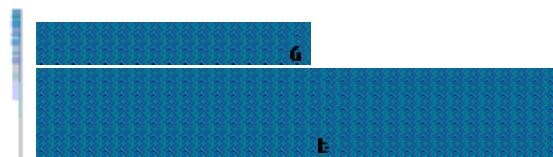
TECHNICAL NOTE 49.2

**Kinetic and stoichiometric analysis of *Rhodospirillum rubrum* growth in
cylindrical photobioreactor at constant incident light flux
- Experimental aspects and preliminary modelling -**

Version 1

Issue 0

L. Favier-Teodorescu, J.-F. Cornet, C.G. Dussap



Document change log

Version	Issue	Date	Observations
0	0	April 2003	Draft version
1	0	June 2003	Final version

Contents

1. SCOPE AND OBJECTIVES OF THE STUDY.....	1
2. MATERIALS AND METHODS	4
2.1. ORGANISM	4
2.2. DEFINITION OF THE CULTURE MEDIA	4
2.2.1. <i>Reviving medium</i>	4
2.2.2. <i>Growth media for flask and reactor cultures</i>	5
2.3. STOCK AND SHAKE FLASK CULTURES.....	7
2.3.1. <i>Stock culture</i>	7
2.3.2. <i>Flask culture</i>	7
2.3.3. <i>Batch and continuous cultures</i>	8
2.4. PHOTOBIOREACTOR AND OPERATING CONDITIONS.....	8
2.5. MEASUREMENT AND CHEMICAL ANALYSIS ON THE LIQUID PHASE OF THE PBR	10
2.5.1. <i>Dissolved carbon dioxide determination</i>	10
2.5.2. <i>Cell dry matter determination</i>	11
2.5.3. <i>Organic acid high pressure liquid chromatography (HPLC) determination</i>	11
2.5.4. <i>Proteins determination</i>	12
2.5.5. <i>Total carbohydrates determination</i>	12
2.5.6. <i>Pigments determination</i>	13
2.5.7. <i>PHB determination</i>	18
3. STOICHIOMETRIC MODEL AND KINETIC LAW	22
3.1. STOICHIOMETRIC MODEL	22
3.1.1. <i>Determination of elemental composition:</i>	22
3.1.2. <i>Stoichiometric model formulation</i>	23
3.2. KINETIC MODELLING.....	25
3.2.1. <i>Radiant light transfer</i>	25
3.2.2. <i>Coupling light transfer with local and spatial kinetic rates</i>	27
3.3. SPATIAL MASS BALANCES.....	30
4. EXPERIMENTAL RESULTS	31
4.1. CONTINUOUS CULTURE TESTS.....	31
4.2. STEADY STATE EXPERIMENTAL DATA CALCULATIONS.....	31
4.3. <i>Rs. rubrum ATCC 25903 GROWN WITH ACETATE IN KINETIC MODE</i>	32
4.4. <i>Rs. rubrum ATCC 25903 GROWN WITH ACETATE UNDER LIGHT LIMITED CONDITIONS</i>	34
5. DISCUSSION	42

5.1. EFFECT OF LIGHT LIMITATION ON BIOMASS CONCENTRATION AND PRODUCTIVITY.....	42
5.2. LIGHT LIMITATION EFFECT ON THE INTRACELLULAR COMPONENT S OF BIOMASS	47
5.3. LIGHT LIMITATION EFFECT ON ELEMENTAL BIOMASS COMPOSITION	49
5.4. VALIDATION OF THE KINETIC MODEL IN TERM OF PRODUCTIVITY.....	50
5.5. VALIDATION OF THE STOICHIOMETRIC MODEL.....	51
6. CONCLUSIONS AND PERSPECTIVES	55
7. REFERENCES	57

1. Scope and objectives of the study

MELiSSA (Micro-Ecological Life Support Alternative) has been conceived as a micro-organism based ecosystem, intended as a tool for understanding the behaviour of artificial ecosystems, and developing the technology for a future biological life support system for long term manned space missions. The loop model was based in the recovery process that can be found in an "aquatic" ecosystem.

The purpose of the loop is to recycle the wastes coming from its main compartment (the crew) and to regenerate its needs.

In its initial design, the MELiSSA loop was based on four axenic compartments colonised by micro-organisms: the *liquefying* compartment, the *phototroph anoxygenic* compartment, the *nitrifying* compartment and the *photosynthetic* compartment. The fifth compartment being the *crew*. However in order to have MELiSSA as a potential BLSS a Higher Plant Chamber working in parallel with the photosynthetic compartment was added to the loop (figure 1).

The implementation of a such system requires the development of a control strategy able to maintain the stability of the loop and to ensure the survival of the crew.

An efficient control of this system requires knowledge models for each of these compartments which can predict the influence of different operating conditions. Consequently, the study and the characterisation of each isolated micro-organisms culture in relation with the environmental conditions is an essential step.

The present work is focused on the second compartment modelling (figure 1) of the MELiSSA loop. Its purpose is the consumption of the products from the degradation activities of the first compartment, mainly represented by fatty acids and carbon dioxide.

Rhodospirillum rubrum was chosen as the most appropriate photoheterotrophic microorganism to convert these products into edible biomass under anaerobic conditions in a closed photobioreactor (PBR).

MELISSA ADVANCED LOOP CONCEPT

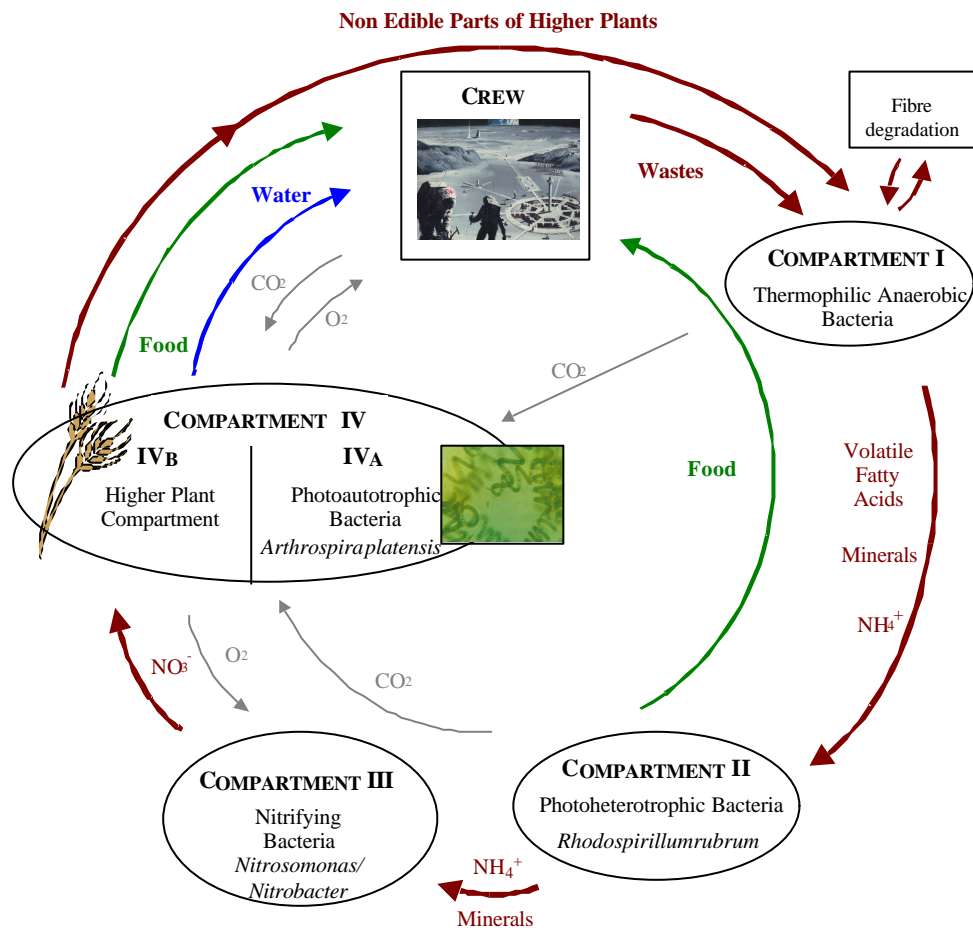


Figure 1: Schematic representation of the MELISSA loop.

Modelling an artificial photobioreactor presents a higher degree of complexity than the conventional bioreactors. The modelisation of a PBR requires to formulate the coupling between the light transfer in the culture medium with the local biomass growth rates and stoichiometries. The difficulty results also from the heterogeneity of the radiation field inside the vessel (Cornet *et al.*, 1998) determined by the absorption and scattering of light by the cells.

The aim of this Technical Note is to study the relationship between the incident light limitation and the *Rs. rubrum* growth kinetics under photoheterotrophic conditions with acetate as carbon source.

A proper investigation of this relationship in batch cultures is a difficult task because the biomass concentration increases continuously, affecting the light distribution inside the vessel. By contrast, in continuous cultures steady state conditions for biomass concentration can be achieved. Such conditions are fundamental to study the relationship between biomass productivity and physical phenomenon of light transfer and were retained for the present study.

It must be noted that in the case of continuous photosynthetic cultures, two independent parameters of operation can be varied : the *dilution rate* and the *incident light flux*.

In the present Technical Note, the light distribution inside the culture was modified only by **changing the steady-state biomass concentration while the radiant incident flux was kept constant (100 W/m²)**. A cylindrical, radially illuminated photobioreactor allowing the *Rs. rubrum* culture under anaerobic and fully controlled continuous growth conditions was used for this purpose.

First, we investigated the influence of light limitation on *Rs. rubrum* growth kinetics, metabolic products formation and macromolecular biomass composition (proteins, carbohydrates, PHB and pigments).

Beside this macromolecular composition, attention was also paid to the possible changes in the elemental biomass composition as a function of the light limitation.

This study proposes also a kinetic and a stoichiometric model for the light limited growth of *Rs. rubrum* in continuous culture. The established kinetic approach takes into account the light distribution inside the reactor. Biomass productivities, conversion yields and molar partition of the synthesised products between biomass and carbon dioxide were calculated and then compared to the experimental ones.

2. Materials and methods

2.1. Organism

The experiments presented in this study were performed with purple nonsulfur bacteria *Rhodospirillum rubrum* ATCC 25903 obtained from the American Culture Collection.

2.2. Definition of the culture media

2.2.1. Reviving medium

Rs. rubrum ATCC 25903 was received freeze dried and was revived using an ATCC recommended medium (R8 AH medium, # 550 broth) and procedure. This medium was used only during the reviving phase.

The R8 AH medium composition was the following:

➤ **ATCC R 8 AH medium composition**

Dissolve to 1 liter of distilled water.

○ *Solution A*

Acid malic	2.5
yeast extract	1 g
(NH ₄) ₂ SO ₄	1.25 g
MgSO ₄ 7H ₂ O	0.2 g
CaCl ₂ H ₂ O	0.07 g
Ferric citrate	0.01 g
EDTA	0,02 g
KH ₂ PO ₄	0.6 g
K ₂ HPO ₄	0.9 g
Solution B (traces)	1 ml
Solution C (vitamins)	7.5 ml

○ *Solution B (traces) for 100 ml:*

Ferric citrate	0.3 g
MnSO ₄ H ₂ O	0.002 g

H ₃ BO ₃	0.001 g
CuSO ₄ 5H ₂ O	0.001g
Mo ₇ O ₂₄ 4H ₂ O	0.002 g
ZnSO ₄	0.001g
EDTA	0.05 g
CaCl ₂ 2H ₂ O	0.02 g

○ Solution C (vitamins) for 1 liter :

Acid nicotinic	0.2 g
Nicotine amide	0.2 g
Thiamine	0.4 g
Biotin	0.008 g

Remarks:

All the solutions were prepared with distilled water. The pH of the prepared ATCC R8 AH media was adjusted at 6.9 with a 5N NaOH solution before autoclaving. The prepared media was sterilised at 121 °C during 15 minutes. Vitamins were sterilised by filtration (filter Schleicher & Schuell of 0,45 µm, Germany) and added to the prepared media after the sterilisation.

2.2.2. Growth media for flask and reactor cultures

The culture medium used during all the experiments contains an excess of all the nutrients essential for *Rs. rubrum* growth. The used media was based on the basal salts mixture of Segers & Verstraete (1983) as described by Suhaimi *et al.* (1987).

Slight modifications were made. The medium was supplemented with acetate and ammonium chloride as the appropriate C and N sources. Biotin was used as the only vitamin. Acetate and NH₄⁺ levels in the prepared media were (3.75 and 1.89 g/l), in order to be in growth conditions where C and N are in excess. For the prepared media the C/N ratio was of 3 (Favier *et al.*, 2003) to prevent a nitrogen limitation. Phosphate concentration was decreased at KH₂PO₄ 0.49 g/l and respectively at K₂HPO₄ 0.52 g/l.

In order to prevent the formation of a precipitate, the medium components were divided in two groups (see below). The pH of the solutions (1) and (2) was adjusted to 6.9 with a 5N NaOH solution before autoclaving. The phosphate solution (solution 2) was sterilised separately at 121°C for 20 min and added as post-sterile addition to the solution (1). Vitamins

solution was sterilised by filtration and added to the culture medium as a post-sterile addition (filter Schleicher & Schuell of 0,45 μm , Germany).

The modified medium, called synthetic basal medium (SBM) was used for the maintenance, stock, batch and for the continuous cultures in order to preserve the same environmental conditions between the inoculum and the culture.

The composition of the SBM defined for 1 liter is indicated as follows:

➤ **Synthetic basal medium composition**

Solution 1:

Component	Final concentration in the growth medium	
	(g/l)	(mol/l)
NH ₄ Cl	1.89	0.035
Na ₂ SO ₄	0.54	0.004
EDTA	0.02	$5.34 \cdot 10^{-5}$
MnCl ₂ 4 H ₂ O	0.01	$5.1 \cdot 10^{-5}$
CH ₃ COOH	3.75	0.063
MgSO ₄ 7 H ₂ O	0.2	$8.13 \cdot 10^{-4}$
CaCl ₂ 2 H ₂ O	0.05	$4.74 \cdot 10^{-4}$
Trace elements	1 ml	-

Solution 2:

Component	Final concentration in the growth medium	
	(g/l)	(mol/l)
KH ₂ PO ₄	0.49	$3.53 \cdot 10^{-3}$
K ₂ HPO ₄	0.52	$2.99 \cdot 10^{-3}$
FeSO ₄ 7 H ₂ O	0.02	$7.19 \cdot 10^{-5}$
NaHCO ₃ (*)	0.25	$3 \cdot 10^{-3}$
MOPS (**)	21	0.1

Solution 3: (traces)

Component	Final concentration in the growth medium	
	(g/l)	(mol/l)
NiSO ₄ 6H ₂ O	0.5	$1.9 \cdot 10^{-3}$

ZnSO ₄ 7H ₂ O	0.1	3.48 10 ⁻⁴
CuSO ₄ 5H ₂ O	0.005	2 10 ⁻⁵
H ₃ BO	0.1	6.183
Na ₂ MoO ₄ 2H ₂ O	0.05	2.07 10 ⁻⁴

Solution 4: (vitamins)

Component	Final concentration in the growth medium	
	(g/l)	(mol/l)
Biotin	0.015	6.15 10 ⁻⁵

Table 1 : Detailed composition of the solutions used for the preparation of the synthetic basal medium used for the *Rhodospirillum rubrum* growth in flasks and reactor cultures.

(*) The sodium bicarbonate (NaHCO₃) was used only for the shake-flask, stock and batch cultivations.

(**) The control of the pH in the shake-flask and stock cultivations was achieved by the utilisation of MOPS (3-morpholino-propane sulfonic acid) as organic buffer.

2.3. Stock and shake flask cultures

2.3.1. Stock culture

Rs. rubrum is maintained in basal medium in screw-cap tubes (usually of 20 ml) at the room temperature. An inoculum of 10 % (vol.) was used. Anaerobic growth conditions were achieved by filling up the capped tubes with culture medium. Strain transfer is made every two months.

2.3.2. Flask culture

Preculture was carried out in 500 ml Erlenmeyer flasks containing 250 ml of sterile medium (50 ml of solution (1) and 200 ml of solution (2)). An inoculum of 20 % (vol.) was transferred to the sterile medium. The mouth of each flask was fitted with a rubber stopper carrying input

and output tubes for flushing the culture with argon. The flush time was 15 minutes at the flush rate of 2 sl/min. After gassing the inlet and outlet tubing are closed with Mohr clamps in order to provide anaerobic growth conditions during the growth time.

The flasks were then placed in a thermostatic orbital shaker bath (New Brunswick scientific Co., Inc, N.J., USA; model G76) at 100 rpm at 30°C approximately. The culture were illuminated by 4 cool white fluorescent lamps (Osram, Germany; 4 x 18 W) for 2 weeks (figure 2) under a incident light of 6 W/m².

Flasks cultures are used for routine maintenance of *Rs. rubrum* and for photobioreactor inoculation.

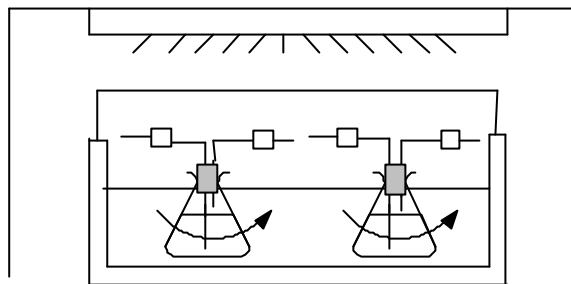


Figure 2: Lightening device for *Rs. rubrum* flask cultures used during this study.

2.3.3. Batch and continuous cultures

Batch and continuous cultures were conducted in a 7 l bioreactor (Aplikon). The reactor was inoculated directly with the axenic culture of two Erlenmeyer flasks.

2.4. Photobioreactor and operating conditions

Cultivation of *Rs. rubrum* was carried out in cylindrical and radially illuminated photobioreactor (figure 3) equipped with two rushton turbines. The used PBR has a radius of 0.08 m and a working volume of 5 l.

A continuous artificial illumination was provided by 55 halogen lamps (Sylvania professional 25 BAB 38°, 12V 20W) arranged around the reactor. Illumination of the culture was fixed to the desired level by fixing the power applied to the halogen lamps. Light incident fluxes calibration was done from a method described elsewhere (Cornet *et al.*, 1997) using a

spherical quantum sensor (Licor Li-190SA) attached to a LI-189 portable meter. A correction is applied for the considered emission spectrum of the lamps in order to obtain a value in the range 350-950 nm.



Figure 3 : Experimental system used for the *Rs. rubrum* photoheterotrophic growth in chemostat mode.

The temperature was controlled and regulated at 30°C by using a water bath with heating and cooling capacities. The pH is controlled and maintained at 7 with H₂SO₄ 1N. Agitation was varied between 200 and 600 rpm. Argon was passed through the medium at a rate of 4 sl/h to provide anaerobic growth conditions.

All the experiments presented in this study were done in continuous mode. The working dilution rate (D) was fixed by adjusting the volumetric flows rate of the input flow of the reactor, the liquid level was maintained at a constant value (5 l) by a capacitive sensor. The feeding solution was stirred with a magnetic bar to supply a homogeneous media to the reactor.

A series of experiments were done at different dilution rates (0.022, 0.042, 0.087, 0.114 h^{-1}), while the incident light flux was kept constant at 100 W/m^2 [350-950 nm]. For each of them, the effect of mixing was investigated by varying the rotation speed of the impeller.

Samples were taken periodically from the output flow to track the changes in the system until a steady state was obtained. This was confirmed by repeated determinations of dry weight, acetate concentration and pigment content. At steady state, the dry weight, acetate concentration and pigment, protein, total carbohydrates and poly- β hydroxybutyric acid (PHB) contents were determined. The carbon dioxide mole fraction in the output gas phase of the reactor is continuously analysed using a CO_2 infrared analyser (ADC, England).

2.5. Measurement and chemical analysis on the liquid phase of the PBR

2.5.1. Dissolved carbon dioxide determination

The dissolved carbon dioxide was quantified by gas balance on the reactor from the knowledge of the volumetric CO_2 gas-liquid mass transfer coefficient preliminary determined (Cornet, 1992). It was calculated according to the mass balance on the total inorganic carbon C_T :

$$C_T = \frac{Y^S_{\text{CO}_2}}{0.186 \cdot K_L a \cdot V_L} \cdot \left[\frac{G_0}{1 - Y^S_{\text{CO}_2}} + K_L a \cdot \frac{P_T}{H} \cdot V_L \right] \quad (1)$$

with:

$Y^S_{\text{CO}_2}$ - carbon dioxide molar fraction in the outlet gas of the reactor;

G_0 - gas molar flow rate (mol/h);

P_T - total pressure (atm);

H - Henry's constant for CO_2 (l atm /mol);

V_L - reactor working volume (l);

$K_L a$ - volumetric mass transfer coefficient (h^{-1});

C_T - total inorganic carbon concentration (mol/l).

C_T is defined as follows: $C_T = C_{CO_2} + C_{HCO_3^-} + C_{CO_3^{2-}}$ (2)

The volumetric mass transfer coefficient is function of the reactor rotation speed (table 2). For CO_2 at a flow rate of 4 sl/h calculation the following $K_L a$ values are considered:

Rotation speed (rpm)	$K_L a$ (h^{-1})
200	0.6
400	2
600	8

Table 2 : Volumetric mass transfer coefficient in function of the agitation speed.

2.5.2. Cell dry matter determination

Dry weight of the suspensions was measured gravimetrically with acetate cellulose membrane filters (Schleicher & Schuell Dassel, Alemagne, 404012) with a pore size of 0.45 μm . The filters were dried and weighted. 5-20 ml of bacterial suspension were filtered and washed twice with distilled water to remove the residual medium constituents. The filters were dried in the oven for 24 h at 110°C.

The cell dry matter of the sample s was determined in duplicate.

2.5.3. Organic acid high pressure liquid chromatography (HPLC) determination

Acetate and acetoacetate concentrations in the culture medium were quantified by High Performance Liquid Chromatography (HPLC) from the supernatant of centrifuged samples (5 min at 10000 g).

The used chromatograph *Agilent 1100* is fitted with two ionic exclusion columns (PHENOMENEX REZEX ROA-300 x 7.8 mm) placed in a thermostated oven set at 50 °C. Component detection is provided by a refractometer (HP serie 1100). A 2 mM sulphuric acid solution at a flow rate of 0,7 ml/min was used as eluent. A retention time of acetate and acetoacetate were 27.4 and respectively 25.5 minutes.

For the HPLC calibration acetic and acetoacetic acid solutions with a known concentration were used as standards. An example of HPLC separation of this compounds is presented in figure 4.

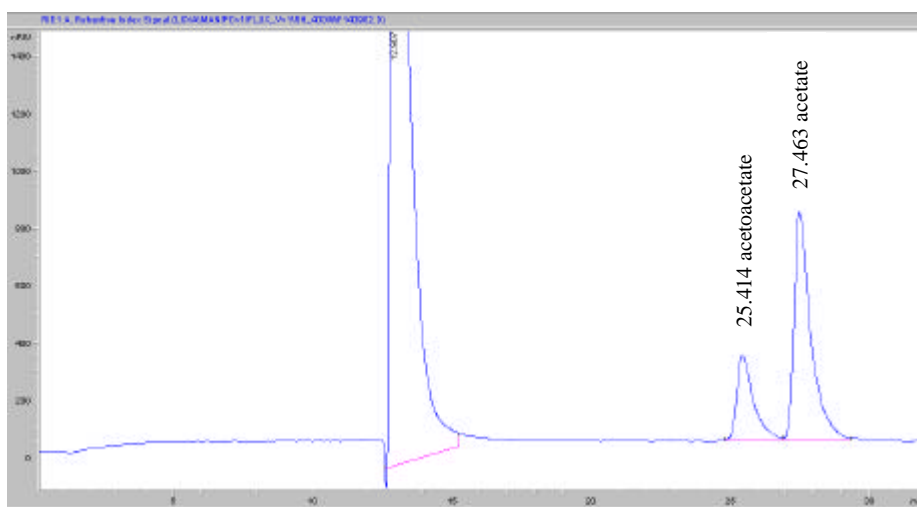


Figure 4: HPLC chromatogram of a solution containing acetate and acetoacetate. The characteristic peaks were indicated in the picture.

2.5.4. Proteins determination

The proteins were determined by the method proposed by Lowry *et al.* (1951) as modified by Peterson *et al.* (1977).

2.5.5. Total carbohydrates determination

Total carbohydrates were determined with the phenol method proposed by Dubois *et al.* (1956) as modified by Herbert *et al.* (1971). The used method and the reagents have the advantage of a great simplicity.

Standard curve was established with a glucose solution of 0.1 g/l.

2.5.6. Pigments determination

In *Rhodospirillaceae* the photosynthetic pigments are located in the cytoplasmic and internal membrane systems. *Rs. rubrum* chromatophores contain bacteriochlorophyll *a* (BChl *a*) as the sole BChl and carotenoids of the spirilloxanthin series, with the spirilloxanthin as the major component.

The bacteriochlorophyll is involved in the reactions that convert the light energy into ATP. Carotenoids are responsible for the bright colour of the purple bacteria and serves as photoprotectants against photo-oxidative damage but also function as accessory photosynthetic pigments involved in transfer of light energy.

In *Rs. rubrum* the carotenoid complex is mainly made by spirilloxanthine (91 %), rhodovibrine (6 %), anhydrorhodovibrine (2 %) and rhodopine (1 %) (Evans *et al.*, 1988).

The photosynthetic pigments can be recognised by their characteristic absorption spectra.

Figure 5 give the absorption spectrum of suspension of intact cells of *Rs. rubrum* after sonication. Different peaks were distinguished:

- the peaks obtained at 375 nm, 590 nm, 800-810 nm, 830-890 nm are characteristic of bacteriochlorophyll *a* (Vredenberg & Ames, 1966);
- the peaks obtained at 486 nm, 515 nm, 552 nm are characteristic of carotenoids (Pfennig & Trüper, 1971).

For pigment estimation, two main peaks corresponding to the absorption maximum for each pigment are retained:

- 884 nm for the bacteriochlorophyll *a*;
- 515 nm for carotenoids.

It must be noted that for this considered peaks, there is no interference between pigment absorption.

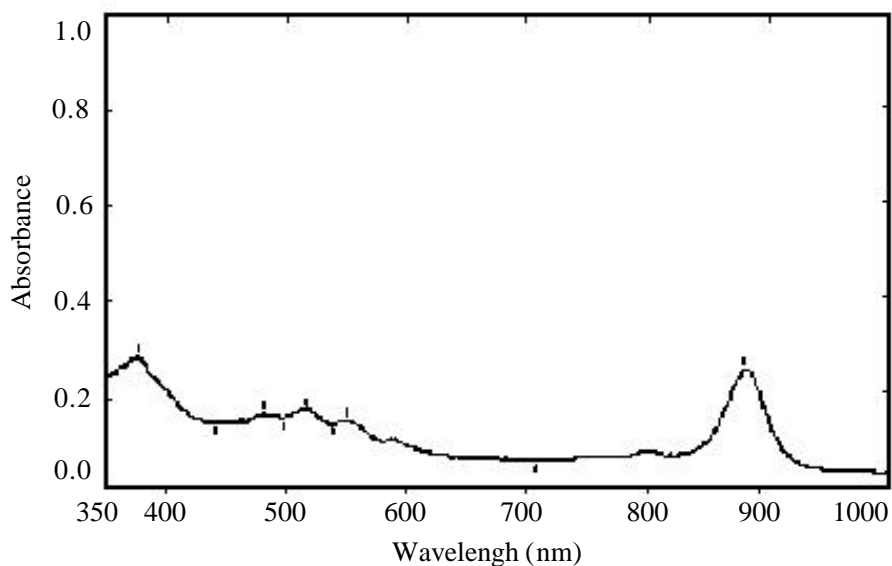


Figure 5: Absorption spectrum of a suspension of intact cells of *Rs. rubrum* after sonication at room temperature recorded on the Shimadzu UV-160A. The cells were taken from flask cultures under anaerobic conditions.

2.5.6.1. Pigments determination by solvent extraction

Different methods were developed for the quantitative determination of bacteriochlorophyll and carotenoids in different purple nonsulphur bacteria suspensions. Generally, all these methods consist in an extraction of the pigments of whole cells suspensions by the addition of an appropriate solvent.

In our work, first, the total amount of bacteriochlorophyll and carotenoid was determined spectrophotometrically after pigment extraction according to the procedure of Cohen-Bazire *et al.* (1957). The extraction step was carried out on fresh (wet) material with a mixture of acetone-methanol. For the pigment quantification, extinction coefficients (ϵ) from the literature were used.

Sample treatment

- ✎ Centrifuge (10 minutes at 16000 g) a volume of bacterial suspension;
- ✎ Resuspend and wash the pellet twice with distilled water;

- ✎ Recentrifuged under the same conditions;
- ✎ Suspended the washed cells under agitation in the same volume of acetone-methanol (7: 2, v/v) solution to extract the pigments from the membrane;
- ✎ Centrifuge (5 minutes at 10000 g) in order to remove the cell wall debris;
- ✎ Measure the absorbancy of the supernatant with a spectrophotometer (Shimadzu UV-160A).

Remark: After the extraction step the pigments determination will be made as soon as possible, since bacteriochlorophyll is relatively unstable in organic solvents, particularly when exposed to light (Cohen-Bazire *et al.*, 1957).

Pigments quantification

Figure 6 show the absorption spectra obtained after pigment extraction with an acetone-methanol solution (7:2 v/v). A shift of the pigment absorption maximum towards the short wavelengths is noted, i.e. for bacteriochlorophyll *a* at 763 nm and for carotenoids at 496 nm after the treatment of the sample with the used solvent.

The bacteriochlorophyll *a* content in the cell was estimated spectrophotometrically by measuring the absorbancy at 763 nm. Its concentration was estimated using an extinction coefficient (ϵ_{772}) of $75 \text{ mM}^{-1} \text{ cm}^{-1}$ or $82.2 \text{ g}^{-1} \text{ L cm}^{-1}$ (Clayton, 1963) according to the formula:

$$C_{BChl\ a} = \frac{OD_{763}}{\epsilon_{772} \times l} \quad (3)$$

where: $C_{BChl\ a}$ is the bacteriochlorophyll *a* concentration in (g/l), OD_{763} is the optical density at 763 nm and l is the optical path length (1 cm).

For the determination of the carotenoid concentration in the extract, the absorbancy of the prepared sample was measured at 496 and 515 nm.

Then, the carotenoid concentration was determined according to the formula:

$$C_{carotenoids} = \frac{OD_{1\ av}}{\epsilon_{1\ av} \times l} \quad (4)$$

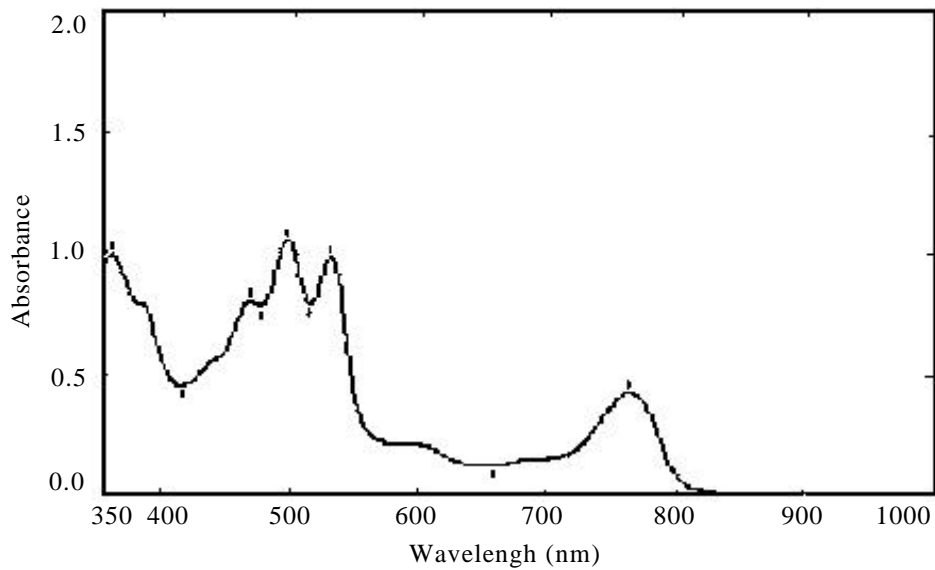


Figure 6: Absorption spectrum of *Rs. rubrum* pure pigments after their extraction with an acetone-methanol solution at room temperature recorded on the Shimadzu UV-160A. The pigments were taken from cell cultures under anaerobic conditions.

An averaged extinction coefficient ($\epsilon_{\lambda_{av}}$) of $250 \text{ g}^{-1} \text{ L cm}^{-1}$ (Liaaen-Jensen & Jensen, 1971) was used for the calculation. It corresponds to absorption maximum between 496 nm and 515 nm.

The $OD_{\lambda_{av}}$ was determined as follows:

$$OD_{\lambda_{av}} = \frac{OD_{496} + OD_{515}}{2} \quad (5)$$

2.5.6.2. Pigment estimation in suspensions of intact cells

The pigments total concentrations are usually determined spectrophotometrically or by HPLC after the pigments extraction in a solvent. Nevertheless, the two methods have different

disadvantages, i.e. incomplete extraction and variable evaporation of acetone during the centrifugation, extraction or during spectrophotometric reading.

In the present study a direct method for the pigment estimation was developed. This method is based on the measurement of the optical density of a whole cells suspension after sonification at two wavelengths 884 nm and 515 nm (corresponding to the absorption maximum of bacteriochlorophyll *a* and carotenoids in vivo).

The cells were pretreated with ultrasounds (IKASONIC U 50 control, IKA Labortechnik) during 2 minutes (0.5 cycle; 70 % of amplitude of the vibrations) in order to break the filaments and to decrease the scattering of the sample.

The spectrum of a *Rs. rubrum* suspension after sonification is presented in figure 5. Measurements of absorbance and whole cell spectra were obtained with a Shimadzu spectrophotometer (model UV-160A).

Optical density corrections

The whole cells scatter much light and thus measured optical densities are not due only to absorption. Thus, the scattering effect could not be neglected for an accurate determination of the real light pigments absorption.

A scattering correction from the OD measurement at 720 nm was made in order to calculate the real absorption of the sample at 884 and respectively at 515 nm.

$$A_{884} = OD_{884} - 0.25 OD_{720}$$

$$A_{515} = OD_{515} - 0.63 OD_{720}$$

It will be noted that the coefficients used for the correction of the optical density at 720 nm were determined according to the Lorenz-Mie theory for scattering.

Relations between concentrations and absorbance

In order to determine the relation between the pigments concentration and the A_{884} and A_{515} the optical density of different *Rs. rubrum* cell suspension were measured at 515, 720 and 884

nm after sonication. Assuming that the pigments concentration is proportional with absorbancy at a given wavelength and using the pigment concentration determined after extraction, the proportionality factors were calculated according to the equation (6) and (7):

$$C_{BChl\ a} = (6.5 \pm 0.8) \times 10^{-3} \times A_{884} \quad (6)$$

$$C_{Carotenoids} = (3 \pm 0.9) \times 10^{-3} \times A_{515} \quad (7)$$

It must be pointed out that, the established coefficients vary significantly from one spectrophotometer to another.

2.5.7. PHB determination

Accurate rapid method for the poly- β -hydroxybutyric acid (PHB) determination is necessary for this study. PHB is a key metabolite involved in energy storage (Dawes & Senior, 1973). For the PHB quantification, the spectrophotometric method of Slepecky & Law (1960) is the widely used. It is based on the conversion of the polymer to crotonic acid by heating with concentrated sulphuric acid. However, this method is extremely time consuming, possess considerable inherent sources of error and is only useful for non-phototrophic organisms because the presence of pigments can interfere with the absorption of the crotonic acid (Brandl *et al.*, 1990).

In this work the formally widely used spectrophotometric method of Law and Slepecky (1960) for quantitative PHB analysis, was replaced by the GC method proposed by Braunegg *et al.* (1978) as modified by Brandl *et al.* (1988). The principle of the used method consist on the intracellular PHB degradation by acidic methanolysis to its constituent β -hydroxybutyric acid methyl esters.

The advantage of the used method is that, only relatively small sample volumes (0.5-5 ml) are required for the analysis. Furthermore, once the sample is collected, all subsequent operations take place in the same screw-capped test tube. Sample preparation is relatively simple involving only the centrifugation and the preparation of the methyl ester derivatives.

Sample preparation

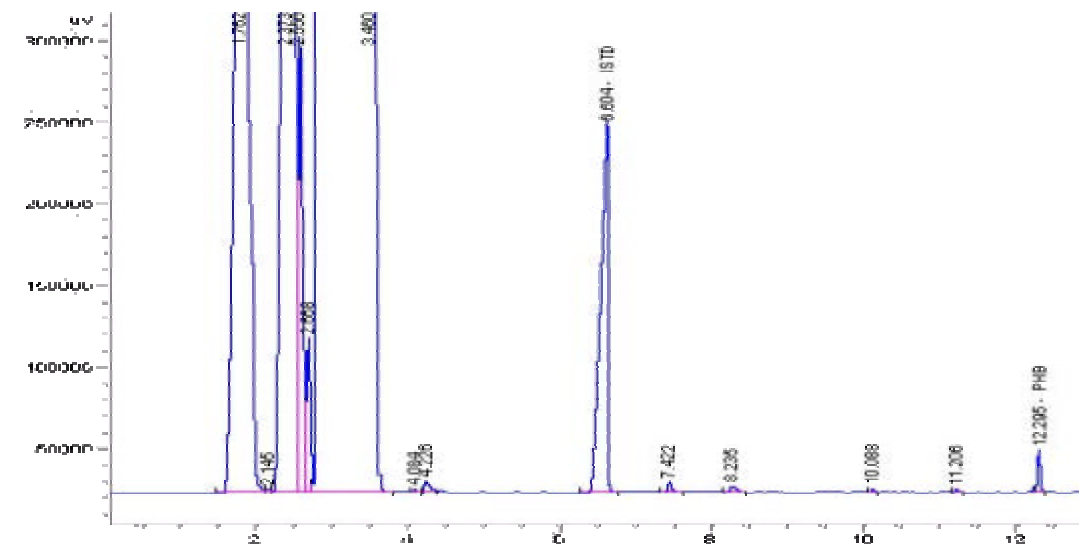
- ✎ Place a volume of bacterial suspension (approximately 2 mg of biomass) in 15 ml Corex tubes;
- ✎ Harvest by centrifugation 10 minutes at 16 400 g;
- ✎ Discard the supernatant;
- ✎ Resuspend and wash once the pellet with distilled water;
- ✎ Centrifuge 10 minutes at 16 400 g;
- ✎ Discard the supernatant;
- ✎ Store the harvested cells in the freezer at -18°C until further processing;
- ✎ React the pellet with 2 ml of acidified methanol solution, i.e. 15% v/v concentrated H_2SO_4 (Brandl *et al.*, 1988) and 2 ml of chloroform;
- ✎ Place screw-capped glass tube of 30 ml;
- ✎ Incubate in a water bath at 100°C for 250 minutes;
- ✎ Cool on ice for 5 minutes;
- ✎ Add 1 ml of distilled water and vortex the whole sample for 1 minute;
- ✎ Centrifuge the treated sample in order to allow the two phases separation;
- ✎ Remove the organic phase (bottom layer) which is to be analysed and transfer to small screw cap glass vials;
- ✎ Store the samples in the freezer at -80°C until further analysis.

Gas-chromatographic analysis of PHB

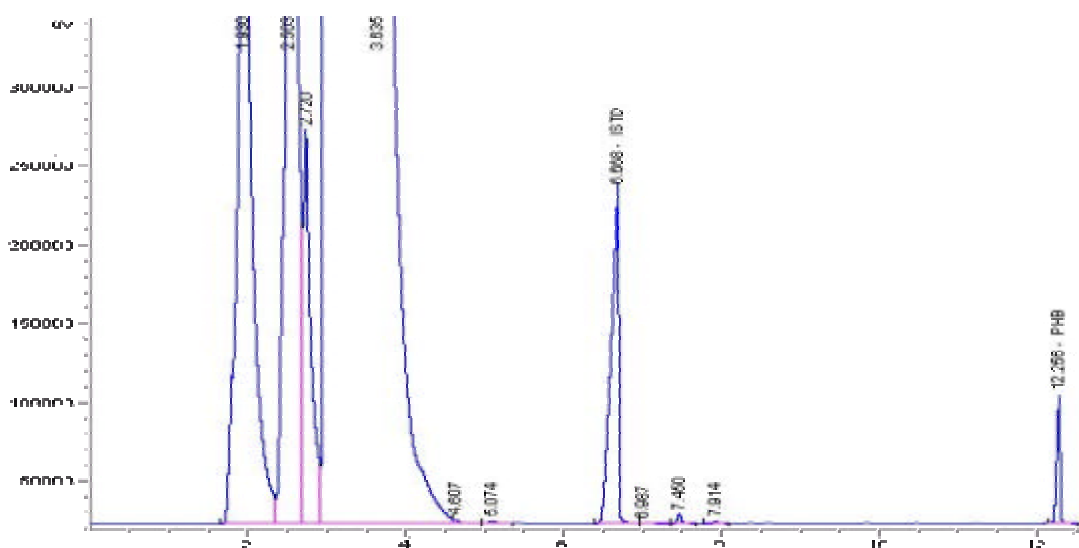
50 μl of organic phase (resulting methyl esters) was quantified by injection in a gas chromatograph (Hewlett Packard HP 6890) equipped with a polar capillary column (30 m by 0.32 mm) (SUPELCOWAX 10; Supelco 2-4084) after splitless injection. For an efficient separation of 3-hydroxybutyric acid methyl esters the following temperature profile for PHB analysis was used 5 minutes at 70°C , followed by a temperature increase rate of $30^{\circ}\text{C}/\text{min}$ at 230°C . Nitrogen is used as carrier gas at a flow rate of 1.7 ml/min and at pressure of 0.78 bar. The temperature of the injector port was set 260°C and that of the flame ionisation detector port was set at 300°C .

Under this conditions a retention time of approximately 6.7 and 12.4 minutes (figure 7) were obtained for the caproic acid and 3-hydroxybutyric acid methyl esters.

The accuracy and the reproducibility of this method were increased by using an internal standard (caproic acid).



(a)



(b)

Figure 7: Gas-liquid chromatogram of 3-hydroxybutyric acid methyl esters obtained by acidic methanolysis method. (a) prepared from poly (3-hydroxybutyric acid) of natural origin; (b) prepared from a PHB synthesised by *Rs. rubrum* grown under anaerobic conditions.

Calibration

Calibration was performed with poly (3-hydroxybutyric acid) of natural origin (Aldrich Chemical Company, Inc., Milwaukee WI 53 233 USA). PHB standards were prepared in the same time as the samples. Figure 8 give an example of calibration curve.

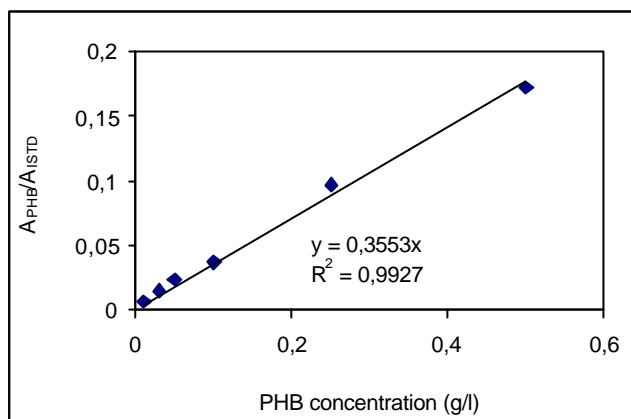


Figure 8: Calibration curve for the gas chromatographic determination of PHB. Different amounts of poly (3-hydroxybutyric acid) of natural origin were treated according to the acidic methanolysis method as described. The concentration of PHB in the sample was plotted versus the ratio areas of peaks of PHB and internal standard (ISTD).

3. Stoichiometric model and kinetic law

Modelling of the photosynthetic bacteria growth is a difficult task. The growth rate is affected by light intensity due to the fact that light is used by this bacteria as energy source.

The complexity of the problem comes from the coupling between the available light inside the reactor with the metabolism of the microorganism. It must be mentioned that a simplified approach is therefore essential to be made.

At ground state, the growth model will contain a single stoichiometric equation and a single kinetic law which considers the phenomenon of light limitation

3.1. Stoichiometric model

3.1.1. Determination of elemental composition:

The previous stoichiometric model (Favier-Teodorescu *et al.*, 1999) proposed for *Rs. rubrum* photoheterotrophic growth considered an elemental composition for biomass obtained from literature data on purple nonsulfur bacteria (Kobayashi & Kurata, 1978). The elemental composition of biomass proposed in this study was : C H_{1.6} O_{0.36} N_{0.222} S_{0.004} P_{0.016}.

The general formulation of the mathematical model was deduced after a detailed description of the metabolic pathways involved in the central metabolism of this bacteria, in the anabolic reactions (synthesis of the constitutive macromolecules from the biomass growth) and in the energetic metabolism (ex: photophosphorylation mechanism) by using the flow calculation method (Favier-Teodorescu *et al.*, 1999 ; Klamt *et al.*, 2002). Stoichiometric equation considers acetate as carbon source, takes into account the consumption of ammonium, sulphates and phosphates and the production of biomass, carbon dioxide and storage products (poly- β -hydroxybutyrate, PHB, is synthesised when the carbon source is acetate) by cells (figure 9).

In this present study, the preliminary approach has been improved by an elemental biomass composition established from independent experimental analysis of the global content of carbon, hydrogen, oxygen, nitrogen, phosphorus and sulphur in *Rs. rubrum* ATCC 25903 dry

matter. The elemental composition of *Rs. rubrum* active biomass has been found to be: $\text{CH}_{1.75}\text{O}_{0.34}\text{N}_{0.188}\text{S}_{0.006}\text{P}_{0.014}$.

The active biomass is defined as the fraction of biomass that ensures the growth and metabolite production (excluding the storage products as PHB).

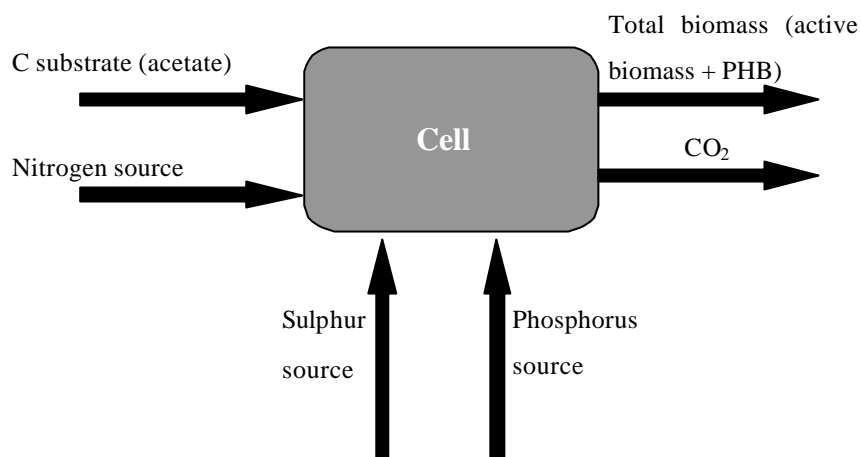
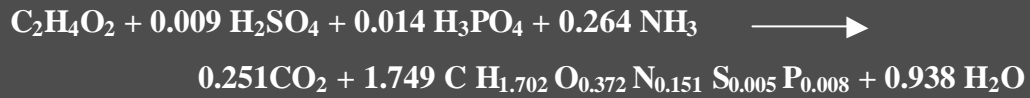


Figure 9: Main flows of substrates and metabolic products considered for the black box stoichiometric model.

3.1.2. Stoichiometric model formulation

It is known that the biomass composition of the photosynthetic micro-organisms changes as a function of external conditions applied (light transfer, carbon source, etc). An extension of the preliminary approach which considers changes in the bacterial composition is then necessary. In order to solve the problem it was assumed that the operating conditions have an influence only on the synthesis of the storage products. Consequently, the elemental active biomass formula was considered to be constant (changes in pigment content does not affect the elemental composition).

To make our reasoning shorter, we have presented in equation (A) only the final reduction of the proposed black box stoichiometry (i.e. after the stoichiometric coefficient identification without any degree of freedom) taking into account a PHB content of 20 % corresponding to the experimental results at an incident light flux of 100 W/m^2 and leading to a respective total biomass C molar formula.



(equation A)

The proposed approach leads to a fixed stoichiometric equation for biomass growth only valid for light limited growth conditions and enables allowance for changes in the total biomass composition (mainly the poly- β -hydroxybutyrate content).

The proposed stoichiometric model was then validated in light limited *Rs. rubrum* continuous cultures at a constant incident radiant energy flux (100 W/m^2) in term of biomass elemental composition and molar carbon partition between synthesised biomass and evolved CO_2 in order to test its applicability.

3.2. Kinetic modelling

3.2.1. Radiant light transfer

The quasi steady state equation of radiative transfer for a non-emitting participating medium (with a and s being respectively the volumetric and scattering coefficients [m^{-1}]):

$$u \cdot \nabla \mathbf{I} = - (a + s) \mathbf{I} + \frac{s}{4\pi} \int_{4\pi} \mathbf{\hat{\omega}} \cdot \mathbf{\hat{\omega}'} I p(\mathbf{\omega}, \mathbf{\omega}') d\mathbf{\omega}' \quad (1)$$

on a given interval of wavelength, may be solved in monodimensional geometries, applying the generalised 2-flux method. The assumption is made that a semi-isotropic intensity distribution exists (and not necessarily an isotropic phase function as for the Schuster-Schwarzschild approach), allowing the integral in equation (1) to be solved for azimuthally symmetric radiation. Thus, the integration on each hemisphere gives the following set of equations in cylindrical coordinates:

$$\begin{cases} \frac{1}{r} \frac{\partial}{\partial r} (r q_r^+) = -(\hat{a} + \hat{s}) q_r^+ + \hat{s} q_r^- \\ \frac{1}{r} \frac{\partial}{\partial r} (r q_r^-) = (\hat{a} + \hat{s}) q_r^- + \hat{s} q_r^+ \end{cases} \quad (I)$$

in which the radiative flux q is defined by the integral over all the directions (solid angle $\mathbf{\omega}$)

$$q = \iint_{4\pi} I \cos \theta d\omega \quad \text{and the total radiant energy available } I_{\Sigma} \text{ by } I_{\Sigma} = \iint_{4\pi} I d\omega$$

The \hat{a} and \hat{s} quantities denote hemispherically integrated values defined by:

$$\begin{aligned} \hat{a} &= 2a = 2EaC_x \\ \hat{s} &= 2bs = 2bEsC_x \end{aligned} \quad (2)$$

in which the back-scattered fraction b is evaluated from the generalised Lorenz-Mie theory (giving $\mathbf{m} = \cos \mathbf{q}$) by the integral of the phase function p (Brewster & Tien, 1982; Koenigsdorff *et al.*, 1991):

$$b = \int_{-1}^0 p(\mathbf{m}, \mathbf{m}) d\mathbf{m} \quad (3)$$

From the Lorenz-Mie theory and using anomalous diffraction approximation (Van de Hulst, 1981) the mean following coefficients have been calculated in the range of wavelength [350-950 nm] for *Rhodospirillum rubrum*:

$$Ea = 154 \text{ m}^2/\text{kg}$$

$$Es = 1348 \text{ m}^2/\text{kg}$$

$$b = 0.0107$$

The resolution of the system of equations (I) with the appropriate boundary conditions corresponding to a mean homogeneous radial incident flux at R $q_R^+ = q_R$ then leads to:

$$\frac{I_{\Sigma r}}{q_R} = \frac{R}{r} \frac{4 \cosh(\mathbf{d} r)}{\cosh(\mathbf{d} R) + \mathbf{a} \sinh(\mathbf{d} R)} \quad (4)$$

and

$$\frac{q_r}{q_R} = \frac{R}{r} \frac{2\mathbf{a} \sinh(\mathbf{d} r)}{\cosh(\mathbf{d} R) + \mathbf{a} \sinh(\mathbf{d} R)} \quad (5)$$

enabling to calculate the profile of total available radiant energy I_S versus the radius r of the PBR, knowing:

$$\alpha = \sqrt{\frac{\hat{a}}{\hat{a} + 2\hat{s}}}$$

$$\delta = \sqrt{\hat{a}(\hat{a} + 2\hat{s})}$$

3.2.2. Coupling light transfer with local and spatial kinetic rates

- Local coupling:

The local volumetric growth rate r_X is easily deduced from the Local Volumetric Rate of radiant Energy Absorbed A (LVREA) applying 2 yields of conversion:

$$r_X = \mathbf{r}\bar{\mathbf{y}}A = \mathbf{r}\bar{\mathbf{y}}E_a C_x I_\Sigma \quad (6)$$

First, the mean mass stoichiometric quantum yield $\bar{\mathbf{y}}$ [kg/J] (i.e. calculated from a mean wavelength in the considered range [350-950 nm] and for a given emission spectrum of the lamps) appears as quasi-constant in regard to radiant light energy changes. The bar indicates a time-averaged value on the metabolism in order to be able to apply the so-called relations of the thermodynamics of irreversible processes (TIP) in the yield calculation (Dussap, 1988; Cornet *et al.*, 1998), or a metabolic flux network approach (Favier *et al.*, 1999). Considering the mixing time in the PBR as a few seconds (corresponding to the mean time for a cell to gather in all the existing local intensities in the PBR), it clearly appears that the environmental relaxation time (some milliseconds) is much smaller than the considered relaxation time for applying TIP (a minute), and hence, the metabolism inside the cells can be safely considered as frozen with respect to the dynamics of change in radiant light energy conditions. Consequently, these latter mechanisms can be removed from the dynamic description of the system (Roels, 1983) justifying the choice of the thermodynamic relaxation time in averaging $\bar{\mathbf{y}}$. In the same time, this analysis shows that there is no difference for the yield \mathbf{y} to be averaged in time $\bar{\mathbf{y}}$, or in space inside the PBR $\langle \mathbf{y} \rangle$. Moreover, if we compare the TIP relaxation time with the characteristic dynamics for growth (few hours), it appears that the main reactions involved in the thermodynamic analysis of photosynthesis can be considered as operating at pseudo steady-state, justifying *per se* this approach.

At the opposite, if we would consider only the primarily redox reactions of photosynthesis (the so-called Z-scheme for *Spirulina* or **q** scheme for *Rs. rubrum*), it would be clear that the extremely short relaxation times (some nanoseconds) of this system would lead to a pseudo steady-state functioning for the electron transfer reactions in comparison with environmental changes, showing that it probably exists very complex adaptation mechanisms for the

photophosphorylation procedure, that we could only take into account by a transient analysis of the coupling between light transfer and hydrodynamics in the PBR.

In this context, the energetic yield \mathbf{r} [dimensionless] roughly corresponding to the primary efficiency of electrons transfer in antenna and to the energy conversion via the so-called Z scheme for photosynthesis is strongly dependent of the total available radiant light energy I_{Σ} and then appears as a local quantity, giving a physical basis to the definition of a local kinetic rate r_x . The maximum value of this yield \mathbf{r}_M appears at the compensation point for photosynthesis and may be calculated from a thermodynamic treatment of the radiant energy conversion process (Bejan, 1987). At the contrary, a theoretical calculation of the law for changes with radiant light energy available is today an unrealistic challenge, despite some tentative analysis (Paillotin, 1974), and one can postulate an arbitrarily hyperbolic law as:

$$\mathbf{r} = \mathbf{r}_M \frac{K}{K + I_{\Sigma}} \quad (7)$$

giving with equation (6) and explaining the LVREA:

$$r_x = \mathbf{r}_M \bar{\mathbf{y}} E a C_x K \frac{I_{\Sigma}}{K + I_{\Sigma}} \quad (8)$$

The calculated coefficients for the local volumetric biomass growth rate are:

$$\mathbf{r}_M = 0.706$$

$$\bar{\mathbf{y}} = 2.6 \cdot 10^{-8} \text{ kg/J}$$

and the sole coefficient experimentally identified is:

$$K = 25 \text{ W/m}^2, \text{ in the range [350-950 nm]}$$

- Spatial coupling:

The calculation of the mean spatial growth rate $\langle r_X \rangle$ is obtained in accordance with the previous analysis given in TN 45.1 (Cornet *et al.*, 1999) and in the paper of Cornet & Albiol (2000). This approach postulates that it may exist an efficient dark zone in the PBR in which nevertheless, the rate is fixed by the physical conditions occurring inside the working illuminated volume. This assumption could be supported at the metabolic level, by the existence of the Reverse Electron Transfer (RET) mechanism, enabling to synthesise reducing power (NADH₂) for short residence time at obscurity. In the general case (physical limitation by light transfer), the total volume of the reactor is then divided into three parts:

- a volume V_1 at obscurity in which no growth occurs as soon as the residence time is not too long to authorise that a new metabolism takes place ($r_{X1} = 0$);
- a volume V_2 (**b** fraction) corresponding to the dark operative zone in the PBR (RET) with a mean rate fixed by the illuminated zone;
- a volume V_3 (**g** fraction) corresponding to the working illuminated volume in which the local rates r_{X3} are given by equation (8).

The mean growth rate is then given by:

$$\langle r_X \rangle = (1 - \mathbf{b} - \mathbf{g}) \frac{1}{V_1} \iiint_{V_1} r_{X1} dV + \mathbf{b} \frac{1}{V_2} \iiint_{V_2} r_{X2} dV + \mathbf{g} \frac{1}{V_3} \iiint_{V_3} r_{X3} dV$$

with $r_{X1} = 0$; postulating $\frac{1}{V_2} \iiint_{V_2} r_{X2} dV = \frac{1}{V_3} \iiint_{V_3} r_{X3} dV$, and taking into account the possibility to have only an illuminated surface fraction f_I onto the PBR, one obtains:

$$\langle r_X \rangle = f_I (\mathbf{b} + \mathbf{g}) \frac{1}{V_3} \iiint_{V_3} r_{X3} dV \quad (9)$$

Comparisons of equation (9) with different experimental results in cylindrical PBR have led to the simple (and expected ?) result that it is necessary to choose $\mathbf{b} = \mathbf{g}$. Then, the final formula giving the mean growth rate is:

$$\langle r_x \rangle = f_I 2g \frac{1}{V_3} \int_{V_3} r_{x3} dV \quad (10)$$

This formula is correct indeed, only if $\gamma \leq 0.5$ (physical limitation by light transfer), otherwise, equation (9) applies with $\mathbf{b} + \mathbf{g} = 1$ ($\beta \leq 0.5$) showing that in physical limitation, the PBR is 2 times more efficient as in kinetic regime ($\mathbf{g} = 1$).

In both cases, the working illuminated volume V_3 is defined in considering that the minimal radiant light energy available for photosynthesis is:

$$I_{Smin} = 0.6 \text{ W/m}^2$$

Clearly, the calculation of the working illuminated volume by equation (4) may lead to cases where two roots exists. The problem will be treated in the same manner as for *Spirulina platensis* (TN 19.1)

3.3. Spatial mass balances

The dynamic or steady-state behaviour of the total biomass concentration is then calculated applying the overall mass balance inside the PBR (considered as a completely stirred tank reactor):

$$Q_L C_X^0 - Q_L C_X + V_L \langle r_x \rangle = V_L \frac{dC_X}{dt} \quad (11)$$

giving directly for batch cultures:

$$\langle r_x \rangle = \frac{dC_X}{dt} \quad (12)$$

and for a continuous culture without biomass in the feed, the non-linear relation:

$$\langle r_x \rangle - \frac{C_X}{t_R} = 0 \quad (13)$$

4. Experimental results

4.1. Continuous culture tests

To examine the influence of light-limitation on the growth of *Rs. rubrum* in batch culture is a difficult task. This is due to the fact that although a constant incident light flux, the light intensity inside the culture vessel varies with location and with time due to the increase in cell concentration. Thus, in batch culture the growth conditions change continuously and more than one factor can reach a critical concentration. This kind of cultures are useful only to give a global information on the cell growth but are not appropriated to investigate the relationship between light limitation and *Rs. rubrum* kinetics.

By contrast, steady state conditions for biomass concentration, can be achieved using a continuous system thereby allowing the relationship between the biomass productivity and the physical phenomenon of light transfer limitation to be studied because the light is not homogeneously distributed in the culture vessel.

The present work is focused on studying the light limited growth of the purple nonsulfur bacterium, *Rs. rubrum* ATCC 25903 cultivated in chemostat mode. The degree of light limitation in the culture was changed by increasing the steady state biomass concentration at a constant incident light flux ($\sim 100 \text{ W/m}^2$). Only steady-state growth was examined. The tests were performed in a cylindrical PBR radially illuminated at different dilution rates and at different rotation speed (200, 400 and respectively 600 rpm). A dilution rate domain between 0.022 and 0.114 h^{-1} was investigated.

4.2. Steady state experimental data calculations

The biomass productivity, elemental biomass formula, intracellular composition of biomass and dissolved species of the liquid phase (acetate, acetoacetate, CO_2) were determined for each test.

Carbon balance was then checked for each experiment and then the carbon recovery percentage, CRP (defined as the ratio of experimental total carbon produced over total carbon consumed) was calculated. It must be noted that CRP allows to evaluate if all the carbon containing

components involved in the bio-process are correctly identified and analysed. Experiments with satisfying CRP only are presented here and analysed for modelling. From the measurements of the biomass and acetate input and output concentrations the mass acetate-biomass yield ($Y_{X/S}$) was calculated as grams of biomass C_x produced per grams of acetate consumed. Molar balance was also checked for each performed test allowing to establish the molar partition of carbon between synthesised biomass and the evolved carbon dioxide.

It must be noted that in the present study all the presented results were obtained by averaging many samples over at least 6 residence times in the PBR.

4.3. *Rs. rubrum* ATCC 25903 grown with acetate in kinetic mode

Test1:

The first continuous experiment was performed at 100 W/m^2 and at a high dilution rate of 0.114 h^{-1} . The prepared culture media contain 3.75 g/l acetic acid and 0.76 g/l NH_4Cl . The C/N ratio of 3. Agitation was fixed at 200 rpm.

For this experiment performed at a high dilution rate and consequently at low biomass concentration, the available light energy exceed the maximum light required for the growth, then all the vessel volume participates to the reaction. In this conditions the working illuminated fraction γ defined as fraction of the total volume which is illuminated is equal to 1.

Thus, the *Rs. rubrum* growth occurs in kinetic mode and the cell productivity depends on the biomass growth kinetics itself, i.e. is fixed by the dilution rate in continuous mode.

Under this growth conditions the steady state is achieved and a steady state biomass concentration of 0.37 g/l was obtained. This leads to a biomass productivity of 0.042 g/l h . Table 3 presents the elemental biomass formula and the main intracellular biomass components obtained for the bacterial growth in kinetic mode.

Mass and molar carbon balances were shown in table 4. For this test, the average $Y_{X/S}$ was calculated to be 0.67 (g/g) .

Operating parameters			D (h ⁻¹)	γ	Productivity (g/l/h)		elemental biomass formula	intracellular biomass components				
F ₀ (W/m ²)	agitation (rpm)	C _{xth} (g/l)			Min.	Max.		Bachll _a (%)	Carotenoids (%)	PHB (%)	Proteins (%)	Carbohydrates (%)
100	200	0,37	0,114	1		0,042	CH _{1,7404} O _{-0,4953} N _{0,1808} S _{0,0036} P _{0,0173}	0,55	0,25	24	54	8,8

Table 3: Experimental data on productivity, elemental biomass formula and intracellular composition of biomass obtained for *Rs. rubrum* growth in kinetic mode (test 1). A culture medium with acetate 3,75 g/l with a C/N ratio of 3 was used.

		input	output						
Input liquid flow rate		acetate _i (gC/h)	acetate _o (gC/h)	biomass (gC/h)	dissolved CO ₂ (gC/h)	CO _{2 gas} (gC/h)	CRP (%)	Y _{X/S}	
Q _v (l/h)	0,569	0,8381	0,7071	0,1019	0,0068	0,005	86,692	0,660	
biomass (g/l)	0,371	Ac(i) - Ac(o) =	0,1311	biomass+CO ₂ dis+CO ₂ g =		0,1136			
input acetate (g/l)	3,594	Carbon balance (molar) :							
output acetate (g/l)	3,032	input		output					
dissolved CO ₂ (mol/l)	0,001	acetate _i (mol/h)	acetate _o (mol/h)	biomass (mol/h)	dissolved CO ₂ (mol/h)	CO _{2 gas} (mol/h)	% biomass	% CO ₂	CRP (%)
CO ₂ gas (ppm)	379	0,0346	0,0292	0,0085	0,0006	0,0004	89,70	10,30	87,378
		Ac(i) - Ac(o) =	0,0054	biomass+CO ₂ dis+CO ₂ g =		0,0095			

Table 4: Mass and molar carbon balance, calculated yields, CRP, and molar partition of carbon between biomass and evolved carbon dioxide for *Rs. rubrum* growth in kinetic mode (test 1).

4.4. *Rs. rubrum* ATCC 25903 grown with acetate under light limited conditions

In this part we have investigated the light limited growth of *Rs. rubrum*.

It is known that a photobioreactor operates in conditions of physical limitation by the light energy transfer when a dark zone appears in the PBR ($\gamma < 1$). This type of limitation correspond to the most commonly encountered condition during the culture of photosynthetic microorganisms.

Light limitation was obtained in this study by decreasing progressively the dilution rate from 0.114 to 0.022 h⁻¹. For each new growth condition the working illuminated fraction (γ) was determined by model calculation.

Test 2:

This test was done at a dilution rate of 0.087 h⁻¹. The culture medium and agitation conditions were the same as in the previous culture (200 rpm). Under these growth conditions the steady state is achieved and the biomass concentration and productivity were found to be 0.82 g/l and respectively 0.07 g/l h (table 5). The calculated mass yield for the biomass synthesis was 0.56 g biomass/ g acetate (table 6).

Test 3:

This continuous culture was performed at the same dilution rate as the previous one. We investigated here the effect of mixing on the *Rs. rubrum* biomass productivity. The agitation was increased here to 400 rpm. Under such conditions the biomass productivity was about 0.08 g/l h. It appears that mixing conditions have an influence on the bacterial growth. Tables 7 and 8 represent the obtained experimental data and the established mass and molar balances. The calculated $Y_{X/S}$ was of 0.6 g/g.

Test 4:

In present test, the agitation was fixed at 200 rpm and a step in the dilution rate from 0.087 to 0.042 h⁻¹ was made. The same culture media was used as previously. Under this experimental conditions a relatively high biomass concentration (1.55 g/l) was obtained (table 9). The calculated cell productivity was 0.065 g/l h.

From the mass balance an $Y_{X/S}$ of 0.55 g/g (table 10) was determined.

Operating parameters			D (h ⁻¹)	γ	Productivity (g/h)		elemental biomass formula	intracellular biomass components				
F ₀ (W/m ²)	agitation (rpm)	C _{x,th} (g/l)			Min.	Max.		Bachll _a (%)	Carotenoids (%)	PHB (%)	Proteins (%)	Carbohydrates (%)
100	200	0,82	0,087	0,28		0,071	CH _{1,7097} O _{0,3939} N _{0,1679} S _{0,0027} P _{0,0095}	1,09	0,31	19	47	7,6

Table 5: Experimental data on productivity, elemental biomass formula and intracellular composition of biomass obtained in light limited conditions (test 2). A culture medium with acetate (3,75 g/l) with a C/N ratio of 3.

		Carbon balance (mass) :						
		input		output				
Input liquid flow rate		acetate _i (gC/h)	acetate _o (gC/h)	biomass (gC/h)	dissolved CO ₂ (gC/h)	CO _{2 gas} (gC/h)	CRP (%)	Y _{X/S}
Q _v (l/h)	0,437	0,6499	0,3902	0,1878	0,0194	0,016	86,144	0,562
biomass (g/l)	0,815	Ac(i) - Ac(o) = 0,2597		biomass+CO ₂ dis+CO ₂ g = 0,2237				
input acetate (g/l)	3,629							
output acetate (g/l)	2,179							
		Carbon balance (molar) :						
		input		output				
CO ₂ gas (ppm)		acetate _i (mol/h)	acetate _o (mol/h)	biomass (mol/h)	dissolved CO ₂ (mol/h)	CO _{2 gas} (mol/h)	% biomass	% CO ₂
1280	0,0037	0,0269	0,0161	0,0157	0,0016	0,0014	83,97	16,03
		Ac(i) - Ac(o) = 0,0107		biomass+CO ₂ dis+CO ₂ g = 0,0186				

Table 6: Mass and molar carbon balance, calculated yields, CRP, and molar partition of carbon between biomass and evolved carbon dioxide for test 2.

Operating parameters			D (h ⁻¹)	γ	Productivity (g/h)		elemental biomass formula	intracellular biomass components				
F ₀ (W/m ²)	agitation (rpm)	C _{xth} (g/l)			Min.	Max.		Bachll _a (%)	Carotenoids (%)	PHB (%)	Proteins (%)	Carbohydrates (%)
100	400	0,89	0,089	0,25		0,079	CH _{1,7097} O _{0,3939} N _{0,1679} S _{0,0027} P _{0,0095}	1,09	0,37	20	45	5,5

Table 7: Experimental data on productivity, elemental biomass formula and intracellular composition of biomass obtained in the test 3 using a culture medium with acetate (3,75 g/l) with a C/N ratio of 3.

		Carbon balance (mass) :							
		input		output					
Input liquid flow rate		acetate _i (gC/h)	acetate _o (gC/h)	biomass (gC/h)	dissolved CO ₂ (gC/h)	CO ₂ gas(gC/h)	CRP (%)	Y _{X/S}	
Q _v (l/h)	0,441	0,6452	0,3771	0,2073	0,0139	0,022	90,66	0,601	
biomass (g/l)	0,89	Ac(i) - Ac(o) = 0,2681		biomass+CO ₂ dis+CO ₂ g = 0,2431					
input acetate (g/l)	3,566								
output acetate (g/l)	2,084								
		Carbon balance (molar) :							
		input		output					
dissolved CO ₂ (mol/l)		acetate _i (mol/h)	acetate _o (mol/h)	biomass (mol/h)	dissolved CO ₂ (mol/h)	CO ₂ gas (mol/h)	% biomass	% CO ₂	CRP (%)
CO ₂ gas (ppm)	1710	0,0267	0,0156	0,0173	0,0012	0,0018	85,25	14,75	91,38
		Ac(i) - Ac(o) = 0,0111		biomass+CO ₂ dis+CO ₂ g = 0,0203					

Table 8: Mass and molar carbon balance, calculated yields, CRP, and molar partition of carbon between biomass and evolved carbon dioxide for test 3.

Operating parameters			D (h ⁻¹)	γ	Productivity (g/h)		elemental biomass formula	intracellular biomass components				
F _o (W/m ²)	agitation (rpm)	C _{x B} (g/l)			Min.	Max.		Bachll _a (%)	Carotenoids (%)	PHB (%)	Proteins (%)	Carbohydrates (%)
100	200	1,55	0,042	0,14		0,065	CH _{1,7258} O _{0,3526} N _{0,1761} S _{0,0033} P _{0,0093}	1,565	0,44	21	46	7,2

Table 9: Experimental data on productivity, elemental biomass formula and intracellular composition of biomass obtained in the test 4 using a culture medium with acetate (3,75 g/l) with a C/N ratio of 3.

		Carbon balance (mass) :							
		input		output					
		acetate _i (gC/h)	acetate _o (gC/h)	biomass (gC/h)	dissolved CO ₂ (gC/h)	CO _{2 gas} (gC/h)	CRP (%)	Y _{X/S}	
Input liquid flow rate	0,441	0,3158	0,0716	0,1748	0,0127	0,022	85,773	0,553	
biomass (g/l)	0,89	Ac(i) - Ac(o) = 0,2442		biomass+CO ₂ dis+CO ₂ g = 0,2094					
input acetate (g/l)	3,566								
output acetate (g/l)	2,084								
		Carbon balance (molar) :							
		input		output					
		acetate _i (mol/h)	acetate _o (mol/h)	biomass (mol/h)	dissolved CO ₂ (mol/h)	CO _{2 gas} (mol/h)	% biomass	% CO ₂	CRP (%)
dissolved CO ₂ (mol/l)	0,003	0,0131	0,0030	0,0146	0,0011	0,0018	83,48	16,52	86,452
CO ₂ gas (ppm)	1710	Ac(i) - Ac(o) = 0,0101		biomass+CO ₂ dis+CO ₂ g = 0,0175					

Table 10: Mass and molar carbon balance, calculated yields, CRP, and molar partition of carbon between biomass and evolved carbon dioxide for test 4.

Test 5:

Similar experiment was also run as previously ($D = 0.042 \text{ h}^{-1}$). At this dilution rate we have investigated again if mixing affects the cell productivity. So, the rotation speed was fixed at 600 rpm. An increase in the biomass concentration, 1.98 g/l occurs and a cell productivity of 0.083 g/l h was obtained.

This demonstrate that in light limitation, mixing time affects the biomass productivity in the PBR. Tables 11 and 12 give the experimental results for this continuous culture. The calculated $Y_{X/S}$ was 0.61 g/g.

Test 6 :

In this test the dilution rate was decreased at 0.022 h^{-1} and the rotation speed was 200 rpm. For this experiment acetate and NH_4Cl concentrations in the PBR were adjusted to 6 g/l and respectively to 3.03 g/l in order to avoid the C and N limitation. The same C/N ratio in the culture media was then maintained at 3 as in the previous tests.

Under this growth conditions the steady state was never achieved and an oscillating behaviour was observed. Consequently, spontaneous oscillations the biomass and acetate concentration in the output flow of the PBR were observed. In this period the cell concentration changes significantly from 1.6 to 3.2 g/l and acetoacetate was alternatively accumulated in the culture medium.

Under this growth conditions the biomass productivities vary between 0.037 and 0.074 g/l h.

Tables 13 and 14 shows the obtained results under this growth conditions. The mass averaged yield for the biomass synthesis was 0.53 g/g.

It must be noted that under this growth conditions a modification of the cell morphology was also observed.

Test 7 :

This test is done in similar conditions to those of test 6. The rotation speed was fixed at 400 rpm. However, at this dilution rate the steady state cell concentration was never achieved and the biomass oscillates between 2 and 4 g/l h (table 15). Thus, the cell productivity oscillates also during the period from 0.044 to 0.089 g/l h (table 16). An $Y_{X/S}$ of 0.56 g/g was calculated.

Operating parameters			D (h ⁻¹)	γ	Productivity (g/l/h)		elemental biomass formula	intracellular biomass components				
F ₀ (W/m ²)	agitation (rpm)	C _{xth} (g/l)			Min.	Max.		Bachll _a (%)	Carotenoids (%)	PHB (%)	Proteins (%)	Carbohydrates (%)
100	600	1,98	0,042	0,11		0,083	CH _{1,7334} O _{0,3788} N _{0,1598} S _{0,0033} P _{0,0078}	1,35	0,46	20	52	6,4

Table 11: Experimental data on productivity, elemental biomass formula and intracellular composition of biomass obtained in the test 5 using a culture medium with acetate (3,75 g/l) with a C/N ratio of 3.

		Carbon balance (mass) :							
		input		output					
Input liquid flow rate		acetate _i (gC/h)	acetate _o (gC/h)	biomass (gC/h)	dissolved CO ₂ (gC/h)	CO ₂ gas (gC/h)	CRP (%)	Y _{X/S}	
Q _v (l/h)	0,209	0,3091	0,0306	0,2225	0,0061	0,028	92,207	0,611	
biomass (g/l)	1,981	Ac(i) - Ac(o) = 0,2785		biomass+CO ₂ dis+CO ₂ g = 0,2568					
acetate input (g/l)	3,6								
acetate output (g/l)	0,356								
dissolved CO ₂ (mol/l)	0,0024	Carbon balance (molar) :							
		input		output					
CO ₂ gas (ppm)	2200	acetate _i (mol/h)	acetate _o (mol/h)	biomass (mol/h)	dissolved CO ₂ (mol/h)	CO ₂ gas (mol/h)	% biomass	% CO ₂	CRP (%)
		0,0128	0,0013	0,0185	0,0005	0,0024	86,63	13,37	92,937
		Ac(i) - Ac(o) = 0,0115		biomass+CO ₂ dis+CO ₂ g = 0,0214					

Table 12: Mass and molar carbon balance, calculated yields, CRP, and molar partition of carbon between biomass and evolved carbon dioxide for test 5.

Operating parameters			D (h ⁻¹)	γ	Productivity (g/lh)		elemental biomass formula	intracellular biomass components				
F _o (W/m ²)	agitation (rpm)	C _{x-ff} (g/l)			Min.	Max.		Bachll _a (%)	Carotenoids (%)	PHB (%)	Proteins (%)	Carbohydrates (%)
100	200	3,2	0,023	0,0625	0,037	0,074	CH _{1,7557} O _{0,4069} N _{0,1416} S _{0,0022} P _{0,0069}	1,52	0,34	20	46	7,1

Table 13: Experimental data on productivity, elemental biomass formula and intracellular composition of biomass obtained in the test 6 using a culture medium with acetate (6 g/l) with a C/N ratio of 3.

		Carbon balance (mass) :									
		input		output							
Input liquid flow rate		acetate _i (gC/h)	acetate _o (gC/h)	biomass (gC/h)	acetoacetate (gC/h)	dissolved CO ₂ (gC/h)	CO _{2, gas} (gC/h)	CRP (%)	Y _{X/S}		
Q _v (l/h)	0,115	0,2568	0,0594	0,1350	0,0073	0,0073	0,024	87,872	0,529		
biomass (g/l)	2,216	Ac(l) - Ac(o) = 0,1973		biomass+CO _{2,dis} +CO _{2,g} =			0,1734				
acetate input (g/l)	5,4479										
acetate output (g/l)	1,261										
acetoacetate output (g/l)	0,1399										
dissolved CO ₂ (mol/l)	0,0053	Carbon balance (molar) :									
CO ₂ gas (ppm)	1848,6	input		output							
		acetate _i (mol/h)	acetate _o (mol/h)	biomass (mol/h)	acetoacetate (mol/h)	dissolved CO ₂ (mol/h)	CO _{2, gas} (mol/h)	% biomass	% CO ₂	% Acetoacetate	CRP (%)
		0,0106	0,0025	0,0113	0,0006	0,0006	0,0020	77,80	17,81	0,04	89,046
		Ac(l) - Ac(o) = 0,0082		biomass+CO _{2,dis} +CO _{2,g} =			0,0145				

Table 14: Mass and molar carbon balance, calculated yields, CRP, and molar partition of carbon between biomass and evolved carbon dioxide for test 6.

Operating parameters			D (h ⁻¹)	γ	Productivity (g/l/h)		elemental biomass formula	intracellular biomass components				
F ₀ (W/m ²)	agitation (rpm)	C _{xth} (g/l)			Min.	Max.		Bachll _a (%)	Carotenoids (%)	PHB (%)	Proteins (%)	Carbohydrates (%)
100	400	2 à 4	0,0222	0,055	0,044	0,089	CH _{1,7557} O _{0,4069} N _{0,1418} S _{0,0022} P _{0,0069}	1,57	0,39	21	50	7,6

Table 15: Experimental data on productivity, elemental biomass formula and intracellular composition of biomass obtained in the test 7 using a culture medium with acetate (7g/l) with a C/N ratio of 3.

		Carbon balance (mass) :									
		input		output							
		acetate _i (gC/h)	acetate _o (gC/h)	biomass (gC/h)	acetoacetate (gC/h)	dissolved CO ₂ (gC/h)	CO _{2, gas} (gC/h)	CRP (%)	Y _{X/S}		
Input liquid flow rate											
Q _v (l/h)	0,111	0,2991	0,0270	0,1963	0,0148	0,0047	0,030	90,171	0,558		
biomass (g/l)	3,336	Ac(l) - Ac(o) = 0,2721		biomass+CO _{2,dis} +CO _{2,g} = 0,2454							
acetate input (g/l)	6,5724										
acetate output (g/l)	0,5925										
acetoacetate output (g/l)	0,2926										
dissolved CO ₂ (mol/l)	0,0035										
CO ₂ gas (ppm)	2300,0										
		Carbon balance (molar) :									
		input		output							
		acetate _i (mol/h)	acetate _o (mol/h)	biomass (mol/h)	acetoacetate (mol/h)	dissolved CO ₂ (mol/h)	CO _{2, gas} (mol/h)	% biomass	% CO ₂	% Acetoacetate	CRP (%)
		0,0124	0,0011	0,0164	0,0013	0,0004	0,0025	79,87	13,88	0,06	91,450
		Ac(l) - Ac(o) = 0,0113		biomass+CO _{2,dis} +CO _{2,g} = 0,0206							

Table 16: Mass and molar carbon balance, calculated yields, CRP, and molar partition of carbon between biomass and evolved carbon dioxide for test 7.

5. Discussion

5.1. Effect of light limitation on biomass concentration and productivity

*a) Mixing effect on *Rs. rubrum* biomass concentration and productivity*

In light limited conditions and at a given dilution rate the mixing effect on biomass concentration and productivity was investigated (table 17). It was tested at each dilution rates providing a light-limited mode. Clearly, an increase in cell concentration and productivity of about 20 % is observed when the mixing rate was increased from 200 rpm to 400 or 600 rpm. No significant influence on the obtained steady state biomass was observed when the stirring rate is increased from 400 to 600 rpm.

The obtained data showed that the biomass productivity is not independent of the mixing conditions in the PBR.

As a tentative of explanation, from the data of Cornet (1992) we have calculated the mixing time and the residence time of cells in the working illuminated and dark inefficient fractions. Moreover, the lightening and dark inefficient frequency were also estimated (Table 18).

Clearly the proposed calculations were not sufficient to give an explanation of the influence of mixing on the determined productivities at different dilution rate. The mechanism involved in this process seems very complex and related to dynamic changes on the redox electron transport chain of photosystem. Further experiments will be necessary for a better understanding of the influence of hydrodynamics on *Rs. rubrum* growth, but is important to retain that mixing influences the definition of the dark operative zone β . The assumption of the model $\beta = \gamma$ then appears only valid at highest productivities i.e., when the optimal conditions of mixing are satisfied.

*b) Effect of the dilution rate on *Rs. rubrum* productivity*

The effect of growth conditions on the biomass concentration and productivity were shown in table 17. For each performed experiment the working illuminated fraction was defined by considering the minimal radiant light energy available for photosynthesis $I_{\Sigma\min}$ and it was determined by model calculation.

When *Rs. rubrum* growth occurs in kinetic mode, i.e. working illuminated fraction of 1, a low biomass concentration (0.37 g/l) was obtained in the PBR. A relatively small productivity of 0.042 g/l h was obtained under these conditions.

As seen in table 17 light limited growth (decreasing in working illuminated fraction) has a clear influence on the cell concentration in the PBR. These data show that a decrease in the dilution rate from 0.87 to 0.022 h⁻¹ was accompanied by an increase of the biomass concentration from 0.9 to 4 g/l. However, under these conditions the resulting biomass productivities appeared in the same range of accuracy.

This findings suggest that apparently the modification of the working illuminated fraction (γ) has no significant effect on biomass productivity whereas the limiting step is the light energy provided at a constant incident flux.

These experimental results confirm the behaviour described earlier by Cornet *et al.* (1998) and Cogne *et al.* (2001) for the cyanobacteria *Arthrospira platensis*, showing that the biomass productivity becomes independent on both the working illuminated fraction and the dilution rate under physical light limitation in a PBR. Moreover, in light limitation the PBR becomes 2 times more efficient as in kinetic regime. One possible explanation is the existence of a dark efficient zone (designated in the model as β fraction of the culture volume) in the PBR as was postulated by Cornet & Dussap (2000; TN 45.5); Cornet & Albiol (2000) for the photoheterotrophic growth of *Rs. rubrum*. The acetate fixation and bacterial growth in this zone are possible as a result of storage of light energy by the micro-organism in the illuminated zone (γ fraction).

Because the mean productivity in the light limitation is twice the productivity observed in kinetic mode ($\gamma = 1$) our experimental results clearly confirm the postulated assumption that the dark efficient fraction is equal to the working illuminated one ($\gamma = \beta$).

In accordance with the presented results it seems that the presence of the dark zone in the PBR is not necessarily negative and correspond to a biological need for *Rs. rubrum* photosynthetic recover.

Radiant incident flux, F_0 (W/m^2)	Agitation (rpm)	Biomass concentration $C_{x,max}$ (g/l)	Working illuminated fraction (g)	Dilution rate D (h^{-1})	Productivity, P (g/l h)	
					Min.	Max.
100	200	0.37	1	0.114		0.042
	200	0.82	0.28	0.087		0.071
	400	0.89	0.25	0.089		0.079
	200	1.55	0.14	0.042		0.065
	600	1.98	0.11	0.042		0.083
	200	3.20	0.0625	0.022	0.037	0.074
	400	4.00	0.055	0.022	0.044	0.089

Table 17: Effect of light limitation on steady state biomass concentration and productivity of continuous cultures of *Rs. rubrum* on acetate in cylindrical radially illuminated photobioreactor and at a constant radiant incident flux, $F_0 = 100 W/m^2$.

Dilution rate D (h^{-1})	Rotation speed (rpm)	Residence time in PBR (h)	Mixing time in PBR (s)	Volume fractions		Residence time in (s)		Frequency (Hz)		Productivity (g/lh)
				γ	$1-\gamma-\beta$	$T_{rv}^{(a)}$	$T_{rd}^{(b)}$	$f_v^{(c)}$	$f_d^{(d)}$	
0.114	200	8.77	7.5	1	0	7.5	-	∞	-	0.042
0.089	200	11.29	7.5	0.28	0.44	2.1	3.3	0.04	0.06	0.071
	400	11.29	3.75	0.25	0.5	0.94	1.88	0.07	0.13	0.079
0.042	200	23.8	7.5	0.14	0.72	1.05	5.4	0.02	0.1	0.065
	600	23.8	2.5	0.11	0.78	0.28	1.95	0.05	0.3	0.083
0.022	200	45.45	7.5	0.0625	0.875	0.469	6.56	0.01	0.12	0.037 - 0.074
	400	45.45	3.75	0.055	0.89	0.21	3.34	0.02	0.24	0.044 - 0.089

Table 18: Effect of mixing on the residence time and frequency of cells in the working illuminated (γ) and dark inefficient fraction ($1-\gamma-\beta$).

^a residence time of cells in the working illuminated fraction of PBR; ^b residence time of cells in the dark inefficient fraction of PBR; ^c crossing frequency of cells in the working illuminated fraction of PBR; ^d crossing frequency of cells in the dark inefficient fraction of PBR.

c) Oscillating behaviour of *Rs. rubrum* culture at low dilution rates

For light limited cultures done at low dilution rates (0.022 h^{-1}) the situation is more complex, because a deviation of the steady state behaviour was observed. Under these growth conditions high biomass concentrations and productivities were obtained. In this case the cell concentration and productivity oscillate periodically (figure 10).

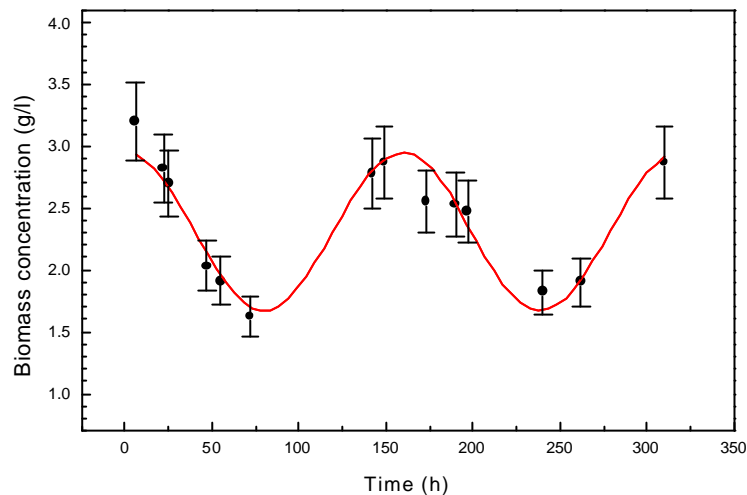


Figure 10: Typical oscillations in *Rs. rubrum* biomass concentration at constant dilution rate ($D = 0.022 \text{ h}^{-1}$).

The last done test has demonstrated that the mixing rate has no effect on this oscillating behaviour but only to the relative productivity. Thus, this growth conditions will represent a major problem for the PBR control and modelling.

At our knowledge it is the first time when a such behaviour is reported for a phototrophic bacterium as *Rs. rubrum* continuously grown in a PBR. Moreover a metabolic modifications and morphological ones were observed during these oscillations. From metabolic point of view it will be noticed that the decrease in biomass growth rate is accompanied by the appearance of acetoacetate production in the output flow of the PBR.

These metabolic changes are also accompanied by morphological changes of the cells leading to very long filaments and lost in cell motility (figure 11).

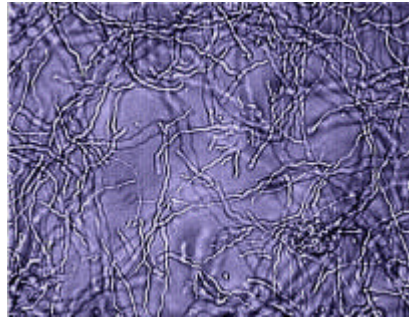


Figure 11: Microscopic observation of *Rs. rubrum* suspension. Image of long non-mobile filaments.

For the differentiation a microscopic observation of cells with normal morphology is presented below.

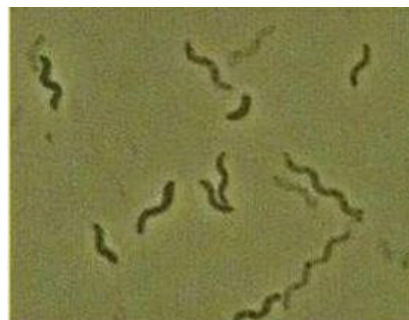


Figure 12: Normal morphology of *Rs. rubrum* cells.

Clearly, the existence of this oscillating behaviour in continuous photoheterotrophic cultures of *Rs. rubrum* performed at low dilution rates is not due to a nutrient limitation as it was reported for *Saccharomyces cerevisiae*. Stable oscillating behaviour was already observed in continuous photoautotrophic cultures of the green eucaryotic unicellular microalga *Chlorella vulgaris* at low dilution rates (Javanmardian & Palsson, 1992 ; Tamy, 1964). However, the mechanism that originates the oscillating behaviour is not clear (Cazzador *et al.*, 1990), although the range of some operating variables which display this behaviour has been investigated.

5.2. Light limitation effect on the intracellular components of biomass

Detailed composition of the main macromolecules of biomass as proteins, carbohydrates, lipids, nucleic acids is required to establish the stoichiometric structured approach for the *Rs. rubrum* growth. Pigment content, which is known to be of little importance on biomass composition, provides however a useful information on light limitation for the light transfer modelling in a PBR. Pigment analysis is therefore required in view to complete our understanding of *Rs. rubrum* growth.

Macromolecules constitute about 96 % of dry weight of bacteria of which about half are proteins. Kobayashi (1995) proposed for the phototrophic bacteria (*Rhodobacter capsulatus*) a macromolecular composition as 60.95 % proteins, 9.91% lipids, 20.83 % soluble carbohydrates and 8.31% other components. However, the relative mass fraction of each main biomass components varies with the cultivation conditions, i.e. it depends on the limiting factor governing the biomass synthesis (light transfer, carbon source concentration, ...). At our knowledge such information for *Rs. rubrum* biomass is not available in the literature data.

The influence of light limitation on biomass macromolecular composition was analysed in this work. Proteins which are the main component in the global biomass were investigated first. Among the components containing carbon in biomass, the carbon storage compounds are those that are known to suffer important changes in function of culture conditions. The purple nonsulfur bacterium, *Rs. rubrum* has been demonstrated to accumulate poly(3 - hydroxybutyrate) (PHB) as intracellular storage material under photoheterotrophic conditions when acetate was used as carbon source (Hustede *et al.*, 1993). For this reason we have also investigated the PHB content in the cells. Then, carbohydrate content in biomass was determined. The *Rs. rubrum* pigments, bacteriochlorophyll *a* (BChl *a*) and carotenoids in the cell material were also measured.

The experimental results obtained for intracellular biomass composition for all the given tests were done in table 19. The presented values are obtained by averaging data from at least 6 residence times and correspond to the steady state for each of the performed cultures.

The obtained results shows that the mass fractions of the main biomass components (proteins, carbohydrates and poly- β -hydroxybutyrate) does not vary significantly with the cultivation conditions (i.e. dilution rate and light limitation) at a constant incident radiant energy flux.

The poly- β -hydroxybutyrate content can be considered as an invariant when the *Rs. rubrum* culture was not limited by carbon, ammonium or phosphate and only related to the incident light flux on the PBR.

Conversely, it seems that light limitation increased the bacteriochlorophyll *a* content in the biomass from 1.1 to 1.6 % instead of 0.55% reached for the *Rs. rubrum* growth in kinetic mode.

Test	Dilution rate D (h ⁻¹)	Working illuminated fraction (γ)	Agitation (rpm)	intracellular biomass components (% DW)					
				BChl _a	Carot. ^(a)	T pigm. ^(b)	PHB	Proteins	Carbohydrates
1	0.114	1	200	0.55	0.25	0.8	24	54	8.8
2	0.087	0.28	200	1.09	0.31	1.4	19	47	7.6
2	0.089	0.25	400	1.09	0.37	1.5	20	45	5.5
4	0.042	0.14	200	1.57	0.44	2.0	21	46	7.2
5	0.042	0.11	600	1.35	0.46	1.8	20	52	6.4
6	0.022	0,0625	200	1.52	0.34	1.9	20	46	7.1
7	0.022	0,055	400	1.57	0.39	2.0	21	50	7.6

Table 19: Effects of the light limitation on the intracellular biomass components content measured in *Rs. rubrum* light limited continuous cultures grown at constant incident radiant energy flux $F_0 = 100 \text{ W/m}^2$; ^(a) carotenoids; ^(b) total pigments.

Whenever the carotenoids content remains fairly constant except in kinetic mode. According to the obtained results the bacteriochlorophyll *a* synthesis seems sensitive to the dark efficient zone at contrary of the carotenoids. Hence, in kinetic mode ($\beta = 0$) the total pigment content in biomass became 3 times lower than that obtained when β is about 0.11. It seems that this bacteria increases their photosynthetic center units to trap light more efficiently in strong light limited conditions.

Several other authors have reported an inverse relationship between the bacteriochlorophyll *a* content and the illumination intensity (Cohen-Bazire *et al.*, 1957; Fuller *et al.*, 1963; Holt *et al.* 1966). This observation suggests that bacteriochlorophyll *a* synthesis is sensitive to light limitation, indicating likely a photosystem mechanism of regulation as stated earlier by Tsygankov & Laurinavichene (1996) in the continuous culture of *Rhodobacter capsulatus*. Moreover Arheim & Oelze (1983) suggested for *Rs. rubrum*, that light may control specific bacteriochlorophyll contents at two different levels, i.e. bacteriochlorophyll *a* formation and growth.

It was also suggested that an increase in BChl _a content means an increase in size or number of photosynthetic units. Thus, in the further modelling approach we will take into account this aspect because the pigment content is strongly involved in the radiative transfer description, so in the definition of the absorption coefficient of light.

5.3. Light limitation effect on elemental biomass composition

Little information is available in the literature in relation with *Rs. rubrum* elemental biomass composition.

Table 20 gives the global biomass formula obtained for each of the performed experiments.

According to the presented data, no significant variations respective to mass fraction of each element C, H, O, N, S, P are observed for the tests carried out under light limited conditions at different dilution rates.

Test	Dilution rate D (h ⁻¹)	Agitation (rpm)	Working illuminated fraction (γ)	elemental biomass formula					
				C	H	O	N	S	P
1	0.114	200	1	1	1.7404	0.4953	0.1808	0.0036	0.0173
2	0.087	200	0.28	1	1.7097	0.3939	0.1679	0.0027	0.0095
3	0.089	400	0.25	1	1.7097	0.3939	0.1679	0.0027	0.0095
4	0.042	200	0.14	1	1.7253	0.3526	0.1761	0.0033	0.0093
5	0.042	600	0.11	1	1.7334	0.3788	0.1598	0.0033	0.0078
6	0.022	200	0.0625	1	1.7557	0.4069	0.1418	0.0022	0.0069
7	0.022	400	0.055	1	1.7557	0.4069	0.1418	0.0022	0.0069

Table 20: Effect of the dilution rate on elemental composition of the biomass obtained in different *Rs. rubrum* light limited continuous cultures grown on acetate as carbon source and at a constant incident radiant energy flux $F_0 = 100 \text{ W/m}^2$.

It must be noted that this data confirm the assumption made for the *Rs. rubrum* stoichiometric modelling that, in light limited growth the elemental composition of biomass remains constant.

As expected, in non-limited light conditions ($\gamma = 1$), *Rs. rubrum* has however a particular behaviour resulting from an increase of oxygen and phosphorus content in the produced

biomass. This could be caused by polyphosphate accumulation and storage (Lee & Choi 1999) when light is in excess, in order to regulate the ratio $P/2e^-$ in the cells.

Moreover, it must be pointed out that the nitrogen content for the two last experiments in oscillating conditions appears significantly lower. Because in this case the protein content is stable, this could result from a decrease in nucleic acid content in the cells.

An averaged global biomass formula was calculated from the experimental results (tests 3, 5, 7) obtained in light limiting growth conditions ($\gamma < 1$) giving: $C H_{1.733} O_{0.393} N_{0.157} S_{0.003} P_{0.008}$. This formula is in good accordance with the theoretical one determined from the previous stoichiometric model (equation A, paragraph 3.1.2.).

Clearly, the new experimental biomass formula utilisation via the stoichiometric model will increase the model predictability.

5.4. Validation of the kinetic model in term of productivity

The proposed *Rs. rubrum* kinetic model will be validated here in term of biomass productivity as a function of light limitation.

In table 21 the maximum experimental productivities obtained in good conditions of mixing (rotation speed higher than 400 rpm) were compared to the predicted one from model calculations.

This presented data show that, the model calculations were in close agreement with the experimental results since the deviation for each run never exceeds 10 % corresponding to the experimental accuracy. Thus, the proposed kinetic model appears well adapted to predict the maximum steady state cell productivity.

It must be noticed that the kinetic model supposes that the best mixing conditions are achieved in the PBR and then calculates maximum biomass productivities.

The experimental data have clearly demonstrated that hydrodynamics inside the PBR played a key role on the observed biomass productivities. In a near future, more accurate modelling including hydrodynamics aspects will be necessary in order to increase the degree of predictability of the proposed kinetic model.

Dilution rate D (h ⁻¹)	Agitation (rpm)	Working illuminated fraction (γ)	Productivity (P)		Deviation (%)
			(from model)	(experimental)	
0.114	200	1	0.038	0.042 ±0.004	- 10
0.089	400	0.25	0.084	0.080 ±0.008	+ 5
0.042	600	0.11	0.085	0.083 ±0.008	+2
0.022	400	0.055	0.085	0.089 ±0.009	-4

Table 21: Comparison between the biomass productivity calculated by the proposed kinetic model and experimental one for *Rs. rubrum* continuous cultures at $F_0 = 100 \text{ W/m}^2$.

Nevertheless, it must be pointed out that the kinetic mode with $\gamma = 1$ is well predicted by model calculations whereas the rotation speed was only 200 rpm. This confirms that hydrodynamics affects only the dark operative zone when it exists and that non-light limited cultures are not sensitive to mixing conditions.

5.5. Validation of the stoichiometric model

The predictability of the stoichiometric model presented above for *Rs. rubrum* growth in term of mass yield for the biomass synthesis and the molar fractions for carbon partitioning between biomass and carbon dioxide was discussed here. The experimental calculated data were compared then with the theoretical ones.

As previously stated (equation A, paragraph 3.1.2), the proposed stoichiometric equation for biomass synthesis with 20 % of PHB content is:



A summary of the obtained results for each of performed experiments were reported in table 20. The mass yields calculated from the experimental results vary from 0.53 to 0.66 g/g i.e. in the range $0.58 \pm 10\%$. This suggests that this value could be independent of the operating conditions (light limitation and mixing rate). The theoretical value calculated from the stoichiometric model is of 0.65 g/g which is fairly in good agreement with the experimental ones but seems slightly higher, corresponding probably to a mean CRP around 90 %.

For the growth conditions studied here, acetate is partitioned simultaneously for the biomass synthesis and carbon dioxide production. The molar fraction of the evolved carbon dioxide is a sensitive measurement of the metabolic activity.

As a general trend for the *Rs. rubrum* light limited growth when the dark efficient zone exists, the molar fraction of the evolved carbon dioxide appears quasi constant.

For experiments performed at high rotation speed (≥ 400 rpm) in good culture conditions (bold values in Table 22) and in light limitation, the mean value observed of $14 \pm 2\%$ seems in good agreement with the theoretical value of 13 % provided by stoichiometric analysis. At contrary, for lower rotation speed (200 rpm) and lower productivities, the mean value observed seems significantly higher (17 %) indicating a metabolic deviation in accordance with hypothesis of a kinetic effect on the dark operative zone.

Under these growth conditions the proposed stoichiometric model with the experimental elemental biomass formula are not sufficient to predict the theoretical molar partition of the synthesised total carbon. The sole solution is to invoke the production of a new undetected carbon metabolite with a higher degree of reduction than the biomass, or a reduced non carbon component (e.g. hydrogen). However, hydrogen was not detected by CPG analysis of the outlet gas of the reactor. It will be noted that, acetoacetate detected by HPLC analysis is not a good candidate, because its degree of reduction is lower than that of biomass.

Finally, the lowest value (10%) is obtained in kinetic regime ($\gamma = 1$) indicating also that the global stoichiometry is not correct in this condition. Nevertheless a new stoichiometric equation (equation B) can be established with the experimental global C-molar formula obtained experimentally for the *Rs. rubrum* growth in kinetic regime. This global formula showed higher levels in oxygen and phosphorus (table 18) leading to the following stoichiometric equation:



(equation B)

in which the theoretical mole partition for CO₂ appears as 8 % indicating a reasonable agreement with the experimental value of 10 ± 2 %. As previously discussed these levels in oxygen and phosphorus in the biomass could result in a intracellular polyphosphate granules accumulation.

Dilution rate D(h ⁻¹)	Agitation (rpm)	Working illuminated fraction (γ)	Mean mass conversion yield Y _{X/S} (g/g)	Molar balance for produced carbon (%)	
				Biomass	CO ₂
0.114	200	1	0.66 ± 0.07	90	10
0.087	200	0.28	0.56 ± 0.05	84	16
0.089	400	0.25	0.60 ± 0.05	85	15
0.042	200	0.14	0.55 ± 0.06	83	17
0.042	600	0.11	0.61 ± 0.06	87	13
0.022	200	0.0625	0.53 ± 0.07	78	18
0.022	400	0.055	0.56 ± 0.04	72	14

Table 22: Effect of light limitation on the mean mass conversion yields and mole partition of produced carbon between the synthesised biomass and the evolved carbon dioxide. Incident radiant energy flux $F_0 = 100 \text{ W/m}^2$.

6. Conclusions and perspectives

The influence of the degree of light limitation on *Rs. rubrum* growth kinetics and metabolic product formation under photoheterotrophic conditions with acetate as carbon source was experimentally investigated in this work. Light limitation was achieved here by changing the dilution rate at a constant incident light flux.

The results presented in this study showed clearly that the light limitation has no effect on the light-limited *Rs. rubrum* productivity, while the working illuminated fraction (γ) was modified. However, under these growth conditions the obtained productivity is twice the one obtained in kinetic regime ($\gamma = 1$, excess of light energy onto the PBR).

The obtained data have also showed that the biomass productivity depends on the mixing conditions in the PBR. A mixing rate of 200 rpm instead 400 rpm leads to a decrease in biomass productivity of 20 %. In relation the experimental results have demonstrated that the kinetic model assumption taking a dark efficient fraction (β) equal to the illuminated working fraction (γ) was valid only when optimal condition of mixing are satisfied (rotation speed higher than 400 rpm). Nevertheless, further experiments are necessary for a better understanding of the influence of hydrodynamics on the bacterial growth.

The obtained results have pointed out that under photoheterotrophic conditions and at low dilution rates *Rs. rubrum* exhibit an oscillatory behaviour. A modification of cell morphology and an acetoacetate accumulation was observed as a consequence of this metabolic modification.

Growth conditions (light limitation and dilution rate) demonstrated no influence on the mass fraction of the main biomass components (proteins, carbohydrates and PHB), and the carotenoids content remains fairly constant. At contrary, bacteriochlorophyll *a* synthesis is sensitive to light limitation, particularly to the dark efficient zone (β).

Thus in a near future we will focus our attention on developing a modelling approach which considers these aspects.

Elemental biomass formulae obtained does not depend significantly of the degree of light limitation. However, in kinetic mode an increase in the oxygen and phosphorus content was observed which is probably due to a polyphosphate accumulation.

From the experimental data an averaged global biomass formula was also proposed and then used for the *Rs. rubrum* stoichiometric modelling in order to increase its degree of predictability.

A new kinetic and stoichiometric knowledge model has been also proposed in this Technical Note. A generalised two-flux approach was used to solve the equation of radiative transfer in the PBR. It enables to calculate analytical solutions for the available light energy profiles inside the reactor. The optical properties of the medium were obtained theoretically from the Lorenz-Mie theory. This approach was used to define the coupling between the available light energy and both local rates and stoichiometry.

The proposed kinetic model has been validated under light limitation in term of biomass productivity. Particularly, its ability to predict biomass productivities obtained when *Rs. rubrum* growth occurs in good culture conditions (high rotation speed) and in light limitation has been proved. It can also predict the biomass productivity obtained in kinetic mode. The proposed model is not able to predict the surprising oscillating behaviour obtained at low dilution rates. Further modifications are necessary in order to simulate the oscillations in biomass concentration.

It must be noted that the established stoichiometric model gave an accurate calculation for theoretical molar partition of the synthesised total carbon and mass yield for the biomass synthesis only when *Rs. rubrum* growth occurs in the best culture conditions (high rotation speed) and light limitation. Nevertheless, in case of kinetic regime ($\gamma = 1$) it has been shown that a stoichiometry taking into account polyphosphate accumulation could be applied.

In a near future, light limitation in *Rs. rubrum* photoheterotrophic continuous culture at different light energy fluxes and at constant steady state biomass concentration needs also to be investigated. The robustness of the proposed knowledge model will be verified also under these growth conditions.

7. References

- ARHEIM K, OELZE J (1983).** Differences in the control of bacteriochlorophyll formation by light and oxygen. *Arch. Microbiol.* **135**: 299-304.
- BEJAN A. (1987).** Unification of three different theories concerning the ideal conversion of enclosed radiation. *J. Sol. Energy Eng.*, 109: 46-51
- BRANDL H, GROSS RA, LENTZ RW, FULLER C (1988).** *Pseudomonas oleovorans* as a source of poly(β -hydroxyalkanoates) for potential applications as biodegradable polyesters. *Appl. Environ. Microbiol.*, **54**: 1977-1982.
- BRANDL H, GROSS RA, LENTZ RW, FULLER RC (1990).** Plastics from bacteria: Poly(β -hydroxyalkanoates) as natural, biocompatible, and biodegradable polyesters. In: *Advances in Biochemical engineering and biotechnology*. Fiecher A (eds.), Springer-Verlag. 41: 77-93.
- BRAUNEGG G, SONNLEITNER B, LAFFERTY RM (1978).** A rapid gas chromatographic method for the determination of poly- β -hydroxybutyric acid in microbial biomass. *European J. Appl. Microbiol. Biotechnol.*, **6**: 29-37.
- BREWSTER MQ, TIEN CL (1982).** Examination of the two-flux model for radiative transfer in particular systems. *Int. J. Heat Mass Transfer.* **25**: 1905-1907.
- CAZZADOR L, MARIANI L, MARTEGANI E, ALBERGHINA L (1990).** Structured segregated models and analysis of self oscillating yeast continuous culture. *Bioproc. Eng.*, **5**: 175-180.
- CLAYTON RK (1966).** Relation between photochemistry and fluorescens in cells and extracts of photosynthetic bacteria. *Photochem. Photobiol.* **5**: 807-821.

- COGNE G, LASSEUR C, CORNET J-F, DUSSAP C-G, GROS G-B (2001).** Growth monitoring of a photosynthetic micro-organism (*Spirulina platensis*) by pressure measurement. *Biotech. Lett.* **23**: 1309-1314.
- COHEN-BAZIRE G, SISTROM WR, STAINIER RY (1957).** Kinetic studies of pigment synthesis by non-sulfur purple bacteria. *J. Cell. Comp. Physiol.* **49**: 25-68.
- COHEN-BAZIRE G, SISTROM WR, STANIER RY (1957).** Kinetic studies of pigment synthesis by non-sulfur purple bacteria. *J. Cell. Comp. Physiol.* **49**: 25.
- CORNET J-F (1992).** Etude cinétique et énergétique d'un photobioréacteur établissement d'un modèle structuré. Applications à un écosystème clos artificiel. *Thèse de doctorat n° 1989*, Université Paris XI – Orsay, France.
- CORNET J-F, DUSSAP C-G, GROS J-B (1998).** Kinetics and energetics of photosynthetic micro-organisms in photobioreactors. *Adv. Biochem. Eng. Biotech.* **59**: 153-224.
- CORNET J-F, DUSSAP C-G, GROS J-B (1999).** Kinetic modeling of *Rhodospirillum rubrum* growth in rectangular photobioreactors. **TN 45.1**. ESTEC Contract 12923/98/NL/MV.
- CORNET J-F, ALBIOL J (2000).** Modeling photoheterotrophic growth kinetics of *Rhodospirillum rubrum* in rectangular photobioreactors. *Biotechnol. Prog.* **16**: 199-207.
- CORNET J-F, DUSSAP C-G (2000).** Kinetic and stoichiometric analysis of *Rhodospirillum rubrum* growth under carbon substrate limitations in rectangular photobioreactors. **TN 45.5**, ESA/ESTEC contract 13323/98/NL/MV.
- DAWES EA, SENIOR PJ (1973).** The role and regulation of energy reserve polymers in micro-organisms. *Adv. Microb. Physiol.* **10**: 135-266.
- DUBOIS M, GILLES KA, HAMILTON JK, REBERS PA, SMITH F (1956).** Colorimetric method for determination of sugars and related substances, *Anal. Biochem.*, **28**: 350-356.

- DUSSAP C-G (1988).** Etude thermodynamique et cinétique de la production de polysaccharides microbiens par fermentation en limitation par le transfert d'oxygène. *Thèse de Doctorat ès Sciences Physiques n° 409*, Université Blaise Pascal, France.
- FAVIER L, PONS A, POUGHON L (1999).** Stoichiometric analysis of *Rs. Rubrum* growth on different carbon substrates. **TN 45.4.** ESTEC Contract 13323/98/NL/MV.
- FAVIER L, CORNET J-F, DUSSAP C-G (2003).** Modelling continuous culture of *Rhodospirillum rubrum* in photobioreactor under light limited conditions. *Biotech. Lett.* **25**: 359-364.
- FULLER RC, CONTI SF, MELLIN DB (1963).** The structure of photosynthetic apparatus in the green and purple bacteria . In: Bacterial photosynthesis. Gest H, San Pietro A. and Vernon LP eds. Antioch Press, Yellow Springs, Ohio. pp: 76-87.
- HERBERT D, PHIPPS PJ, STRANGE RE (1971).** Chemical analysis of Microbial Cell. In : Methods in microbiology. Norris J.R. and Ribbons D.W. (Ed.), Academic Press New York, London.
- HOLT SC, CONTI SF, FULLER RC (1966).** Effect of light intensity on the formation of the photochemical apparatus in the green bacterium, *Chloropseudomonas ethylicum*, *J. Bacteriol.* **94**: 349.
- HUSTEDE E, STEINBUCHER A, SCHLEGEL HG (1993).** Relationship between the photoproduction of hydrogen and the accumulation of PHB in non-sulphur purple bacteria. *Appl. Microbiol. Biotechnol.*, **39**: 87-93.
- JAVANMARDIAN M, PALSSON BO (1992).** Continuous photoautotrophic cultures of the eukariotic alga *Chlorella vulgaris* can exhibit stable oscillatory dynamics. *Biotech. Bioeng.*, **39**: 487-497.
- KLAMT S, SCHUSTER S, GILLES ED (2002).** Calculability analysis in underdetermined metabolic networks illustrated by a model of the central metabolism in purple nonsulfur bacteria. *Biotech. Bioeng.* **7**: 734-751.

- KOBAYASHI M (1995).** Waste remediation and treatment using anoxygenic phototrophic bacteria. In: Blankenship R.E., Madigan M.T. and Bauer C.E. (eds.). *Anoxygenic photosynthetic bacteria*. Kluwer Academic Publishers, The Netherlands. pp. 1269-1282.
- KOBAYASHI M , KURATA S (1978).** Mass culture and cell utilisation of photosynthetic bacteria. *Process Biochem.* **13**: 27-30.
- KOENIGSDORFF R, MILLER F, ZIEGLER R (1991).** Calculation of scattering fractions for use in radiative flux models. *Int. J. Heat Mass Transfer.* **34**: 2673-2676.
- LEE SY, CHOI J (1999).** Production and degradation of polyhydroxyalkanoates in waste environment. *Waste Management* **19**: 133-139.
- LIAAEN-JENSEN S, JENSEN A (1971).** Quantitative determination of carotenoids in photosynthetic tissues. *Methods enzymol.* **23**: 586-602.
- LOWRY OH, ROSENBROUGH NJ, FARR AL, RALL RJ (1951).** Protein measurement with the Folin phenol reagent. *J. Biol. Chem.* **193**: 265-275.
- PAILLOTIN G (1974).** Etude théorique des modes de création, de transport et d'utilisation de l'énergie d'excitation électronique chez les plantes supérieures. *Thèse de Doctorat ès Sciences n° 1380*, Université Paris XI – Orsay, France.
- PETERSON GL (1977).** A simplification of protein assay of Lowry et coll. which is more general applicable. *Anal. Biochem.* **83**: 346-356.
- PFENNING N, TRUPPER HG (1977).** The *Rhodospirillales* (phototrophic or photosynthetic bacteria. In: Laskin AI, Lechevalier HA (eds.), *CRC Handbook of microbiology*, 2nd ed., CRC Press, Cleveland, vol 1, 119-130.
- ROELS J A (1983).** Energetics and kinetics in biotechnology. Elsevier Biomedical Press.
- SEGERS L, VERSTRAETE W (1983).** Conversion of organic acids to H₂ by *Rhodospirillaceae* to grown with glutamate or dinitrogen as nitrogen source. *Biotech. Bioeng.* **25**: 2843-2853.

- SLEPECKY RA and LAW JH (1960).** A rapid spectrophotometric assay of alpha, beta unsaturated acids and beta-hydroxy acids. *Analytical Chemistry*, **32**: 1697-1699.
- SUHAIMI M, LIESSENS J, VERSTRAETE W (1987).** NH₄⁺-N assimilation by *Rhodobacter capsulatus* ATCC 23782 grown axenically and non-axenically in N and C rich media. *J. Appl. Bacteriol.* **62**: 53-64.
- TAMIYA H (1964).** Growth and cell division of *Chlorella*. In: Zeuthen (eds.). Synchrony in cell division and growth. Interscience Publishers, New York.
- TSYGANKOV AA, LAURINAVICHENE TV (1996).** Influence of the degree of light limitation on growth characteristics of the *Rhodobacter capsulatus* continuous culture. *Biotech. Bioeng.* **51**: 605-612.
- VAN de HULST HC (1981).** Light scattering by small particles. 2nd ed., Dover publications Inc.
- VREDENBERG WJ, AMESZ J (1966).** Absorption bands of bacterochlorophyll types in purple bacteria and their response to illumination. *Biochimica and biophysica acta*, **126**: 244-253.